# Progress Report Year 1

## 4-D High-Resolution Seismic Reflection Monitoring of Miscible $CO_2$ Injected into a Carbonate Reservoir

by

Richard D. Miller
Abdelmoneam E. Raef
Alan P. Byrnes
William E. Harrison

Kansas Geological Survey
University of Kansas
1930 Constant Avenue
Lawrence, KS 66047

Open-file Report 2004-45

September 24, 2004

# **Progress Report Year 1:**
# 4-D High-Resolution Seismic Reflection Monitoring of Miscible $CO_2$ Injected into a Carbonate Reservoir

by
Richard D. Miller, Abdelmoneam E. Raef, Alan P. Byrnes, and William E. Harrison
Kansas Geological Survey
University of Kansas

The objective of this research project is to acquire, process, and interpret multiple high-resolution 3-D compressional wave and 2-D, 2-C shear wave seismic data to observe changes in fluid characteristics in an oil field before, during, and after the miscible carbon dioxide ($CO_2$) flood that began around December 1, 2003, as part of the DOE-sponsored Class Revisit Project (DOE #DE-AC26-00BC15124). Unique and key to this imaging activity is the high-resolution nature of the seismic data, minimal deployment design, and the temporal sampling throughout the flood. The 900 m deep test reservoir is located in central Kansas oomoldic limestones of the Lansing-Kansas City Group, deposited on a shallow marine shelf in Pennsylvanian time.

Permits and access agreements were secured for the 810 shot points and 240 receiver stations that make up the 3.6 $km^2$ 3-D deployment (Figure 1). The design provides uniform 20- to 24-fold coverage across an approximately 600 m x 450 m area centered on the flood pattern from start-up to breakthrough. Moving further away from the $CO_2$ injector, the two water injection wells planned for containment are all within the minimum 12-fold boundary. The 2-D, 2-C shear wave lines intersected near the injection well and extend about 400 m away from the injector. Even if the flood strays significantly from the current expected sweep pattern this 3-D design should provide the necessary offsets, offset distribution, azimuthal control, and fold to monitor the $CO_2$ movement and eventual fate.

Patch design has limited the bin (cell) size to a maximum 10 m × 10 m area while maintaining relatively uniform fold, offset, and azimuthal distributions. Shot lines are perpendicular to receiver lines and staggered to form a modified brick pattern. This pattern made access and movement along shot lines precarious in some areas. This style patch complicates the acquisition (source and receiver deployments), but it provides the optimum traces and trace distribution for each bin.

A 240-channel Geometrics Geode distributed system networked to a StrataVisor NZ acquisition controller recorded the seismic data. A single IVI minivib2 with a prototype high-output Atlas rotary control valve swept five times at each source location. Sweep frequencies for the P-wave survey span from 25 to 250 Hz over a 10 second duration. Receivers were three digital grade 10 Hz Mark Products Ultra2w geophones wired in series with 14 cm oversized spikes. Geophones were planted in a fresh spot but within a half-km of the station location as defined during the baseline and previous three monitor surveys. The three-geophone spread formed a 0.5 m equilateral triangle.

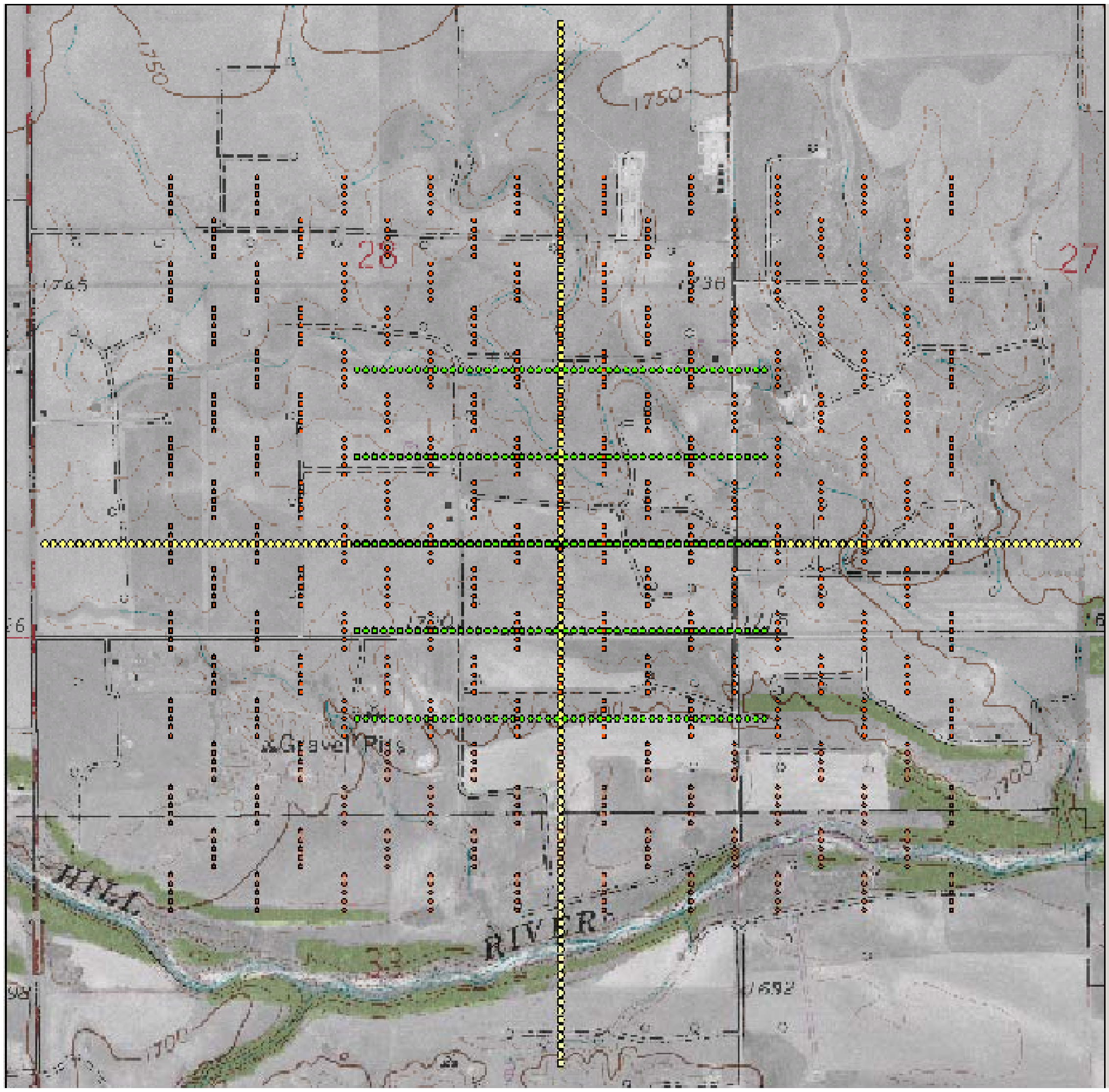


Figure 1. This orthophoto is from the Colliver lease southeast of Russell, Kansas. It is overlain by the current working 3-D compressional and shear wave, high-resolution seismic reflection survey to be acquired 12 times over the next six years. The center of this grid is approximately 20 ft north of the injection well. During a site visit on June 18, 2003, the grid was located with the KGS's Trimble DGPS system. With the grid centered on the $CO_2$ injector, receiver line 4 (forth from the north) was in the center of the east/west county road and receiver line 2 crossed directly through the oil storage tanks and metal building located northwest of the injection well. Site reconnaissance left us with the opinion that with the exception of the shot location in the river and in few of the deeper ditches (approximately 10 to 15), all shot stations should be accessible.

Baseline shear wave data were acquired using an IVI minivib1 with a sweep frequency that ranges from around 15 to 150 Hz and the same seismograph but with 14 Hz horizontal geophones. The spread design and recording parameters were identical to the baseline survey. The resulting data were initially processed in 2-D with follow-up work in 3-D.

Absolute source and receiver location over the 3.6 km$^2$ survey grid were maintained using a Trimble survey-grade DGPS system. The original digital map developed during the baseline survey was used to exactly relocate each station for each of the repeat 3-D surveys.

3-D stacked cubes ready for interpreting were generated using the 2-D/3-D ProMax (a product of Landmark) processing package currently running at the KGS on a dual processor SGI Octane workstation. Refinements to processing flows and reprocessing of previous data sets were continuous throughout year 1. Optimal processing of these 3-D data have involved techniques and algorithms developed for petroleum applications but carefully analyzed and applied in a fashion consistent with the needs of shorter wavelength and lower signal-to-noise ratio high-resolution data. Cross-equalization techniques have not been necessary with the consistency in data acquisition but will be appraised with each new data set.

Interpretation of these seismic data began during year 1. Volumes including instantaneous frequency, amplitude, and phase, along with impedance and coherency, were generated, compared, and differenced in search of the seismic attribute or attributes most sensitive to $CO_2$ (fluid) movement in the reservoir. Successes with instantaneous frequency were observed on initial surveys during year. Landmark's interpretation software Kingdom Suites has proven extremely adaptable to the high-resolution nature of these data and will continue to be the primary interpretation software used during year 2.

**Time Line and Progress**

**Budget Period I. Seismic Design, Pre-injection Survey, and Surveys One - Three.**

**Task One –** Finalize Seismic Survey Design:
(October 2003)

- Subtask 1.1 permits and access
- Subtask 1.2 modify shot and receiver locations based on access
- Subtask 1.3 coordinate with production schemes to minimize noise

**Task Two –** Acquire and Process 3-D Baseline Survey and 2-D Survey:
(November 2003–January 2004)

- Subtask 2.1 GPS survey stations
- Subtask 2.2 standardize procedure for acquisition of 3-D volumes
- Subtask 2.3 acquire 3-D compressional wave baseline survey
- Subtask 2.4 acquire 2-D, 2-C shear wave baseline survey
- Subtask 2.5 generate standard, high resolution 3-D volume
- Subtask 2.6 generate standard, 2-D shear cross-sections (SH & SV)
- Subtask 2.7 preliminary attribute analyses
- Subtask 2.8 compare and contrast with all geologic and reservoir information
- Subtask 2.9 evaluate data quality and potential to achieve goals and objectives

**Task Three –** Develop Synthetic from Reservoir Simulations:
(December 2003–February, 2004)

- Subtask 3.1 run reservoir model forward in time capturing specific snap-shots
- Subtask 3.2 convert simulation output to synthetic using Gassmann's equations

Subtask 3.3 compare and contrast baseline synthetic with real seismic volume
Subtask 3.4 develop optimization scheme to match synthetic and real

**Task Four –** First Time-Lapse 3-D Survey and Correlate to Simulation Prediction:
(January 2004–May 2004)

Subtask 4.1 3-D P-wave survey
Subtask 4.1.1 GPS survey stations
Subtask 4.1.2 acquire 1st 3-D P-wave survey (fixed procedure)
Subtask 4.1.3 process 1st 3-D P-wave survey
Subtask 4.1.4 refine/optimize processing flows, evaluate cross-equalization techniques
Subtask 4.1.5 reprocess both baseline and 1st time lapse using optimized flow
Subtask 4.1.6 attribute analyses
Subtask 4.1.7 evaluate data & likelihood of satisfactorily achieving goals/objectives
Subtask 4.2 Evaluate flood scheme
Subtask 4.2.1 compare differences between synthetic from simulations & real data
Subtask 4.2.2 iteratively revise flood scheme in simulations
Subtask 4.2.3 develop revised flood scheme to min. or eliminate non-linearities

**Task Five –** Second Time-Lapse 3-D Survey and Evaluate Flood Scheme:
(March 2004–July 2004)

Subtask 5.1 3-D P-wave survey
Subtask 5.1.1 GPS survey stations
Subtask 5.1.2 acquire 2nd 3-D P-wave survey (fixed procedure)
Subtask 5.1.3 process 2nd 3-D P-wave survey (fixed flow based on subtask 4.1.4)
Subtask 5.1.4 attribute analysis and interpretation
Subtask 5.2 evaluate flood scheme
Subtask 5.2.1 compare differences between synthetic from simulations & real data
Subtask 5.2.2 iteratively revise flood scheme in simulations
Subtask 5.2.3 develop revised flood scheme to minimize/eliminate non-linearities

**Task Six –** Third Time-Lapse 3-D Survey and Correlate to Simulation Prediction:
(June 2004–September 2004)

Subtask 6.1 3-D P-wave survey
Subtask 6.1.1 GPS survey stations
Subtask 6.1.2 acquire 1st 3-D P-wave survey (fixed procedure)
Subtask 6.1.3 process 1st 3-D P-wave survey
Subtask 6.1.4 refine/optimize processing flows, evaluate cross-equalization techniques
Subtask 6.1.5 reprocess both baseline and 1st time lapse using optimized flow
Subtask 6.1.6 attribute analyses
Subtask 6.1.7 evaluate data & likelihood of satisfactorily achieving goals/objectives
Subtask 6.2 Evaluate flood scheme
Subtask 6.2.1 compare differences between synthetic from simulations & real data
Subtask 6.2.2 iteratively revise flood scheme in simulations
Subtask 6.2.3 develop revised flood scheme to minimize or eliminate non-linearities

| | Budget Period I | Budget Period II | Budget Period III | Budget Period IV | Budget Period V | Budget Period VI |
|---|---|---|---|---|---|---|
| Task | Year 1 2003 - 2004 | Year 2 2004-2005 | Year 3 2005-2006 | Year 4 2006-2007 | Year 5 2007-2008 | Year 6 2008-2009 |
| 1. Seismic survey design | | | | | | |
| 2. Pre-injection 3-D survey | | | | | | |
| 3. Compare simulation to survey ($CO_2$ flood begins) | | | | | | |
| 4. First time-lapse 3-D survey | | | | | | |
| 5. Second time-lapse 3-D survey | | | | | | |
| 6. Third time-lapse 3-D survey | | | | | | |
| 7. Fourth time-lapse 3-D survey | | | | | | |
| 8. Fifth time-lapse 3-D survey | | | | | | |
| 9. Sixth time-lapse 3-D survey | | | | | | |
| 10. Seventh time-lapse 3-D survey | | | | | | |
| 11. Eighth time-lapse 3-D survey | | | | | | |
| 12. Evaluation of flood efficiency | | | | | | |
| 13. Ninth time-lapse 3-D survey | | | | | | |
| 14. Tenth time-lapse 3-D survey ($CO_2$ flood ends) | | | | | | |
| 15. Eleventh time-lapse 3-D survey | | | | | | |
| 16. Final project evaluation and report writing | | | | | | |

## Pre-Survey Preparations

During the June 18, 2003, visit, several key farmers who had land within the grid were contacted. Each expressed a strong interest in the project and willingness to work with us to insure year-around access.

After on-site discussions with a representative from Murfin Drilling (operators of this lease), a location for a semi-permanent monument was established immediately south of the injection well. Once the marker was placed it was located absolutely and was used to definitively locate and deploy the grid each time survey data were acquired.

A digital terrain map was generated using a Trimble DGPS system. Development of a high-resolution digital map of actual shot and receiver locations based on surface access was critical for pre-survey modeling and design. Stations that could not be occupied due to access problems were identified, with new locations (generally offset from the ideal) incorporated into final designs and survey parameters. To minimize the adverse affect of inaccessible stations on fold and azimuthal and offset distribution, it was sometimes necessary to locate replacement stations in particular directions and at specific distances from the receiver grid. For 4-D seismic surveys to be effective it is imperative that each shot and receiver station be accurately reoccupied during each time-lapse 3-D survey, effectively minimizing any changes in the recorded data not related to the injection of $CO_2$. To that end, the digital terrain map provides absolute reoccupation of sources and receivers.

Much of the acquisition on this project was carried out at night to minimize surface noise associated with wind and cultural activities (vehicle traffic). It was imperative that our seismic activities minimally impact current and future agricultural activities within the affected one square mile. With that, a digital tracking log was built to help guide the vibratory source (13,000 lb center articulated, four-wheel-drive vehicle with >3 psi ground pressure) around the site, avoiding fences, ditches, pipelines, etc., and minimizing ground compaction and number of miles traveled through tilled farm fields. With the limited-sight conditions present during many of the first four 3-D surveys, a notebook computer and high-resolution GPS were outfitted for the vibrator, which directed the operator from point to point when weather or night operations permit little or no visibility.

The digital terrain map was constructed using a DGPS mapping system, including a six-wheel-drive ATV, Trimble DGPS, Garmin GPS, and notebook computer (Figure 2). Aided by orthophotos and topo maps, researchers drove and digitally mapped the "best" vibrator route (Figure 3). Key priorities were minimal ground disturbance and best path around obstacles in all weather conditions. The digital mapping system was developed and assembled at the Kansas Geological Survey's fabrication facility specifically for this project. This modular system uses custom software interfaced to two GPS receivers, allowing real time placement and guidance referenced to orthophotos (digital, high-resolution aerophotos) and digital topo maps.

Figure 2.


Figure 3.

A preliminary tracking log provided an overview of the route most easily traversed by the ATV and one that the researchers believed would accommodate the vibrator in all weather (Figure 4). The red lines track the path followed by the digital mapping unit. The blue dots are the ideal shot station locations. With the western two-thirds completed, all but about 10% of the shot stations were easily accessible. Some minor dozer work was necessary to reduce this missing 10% in the western two-thirds down to less than 5%. Once this preliminary mapping was completed, manual editing produced a uniform route with location accuracy around 5 cm.

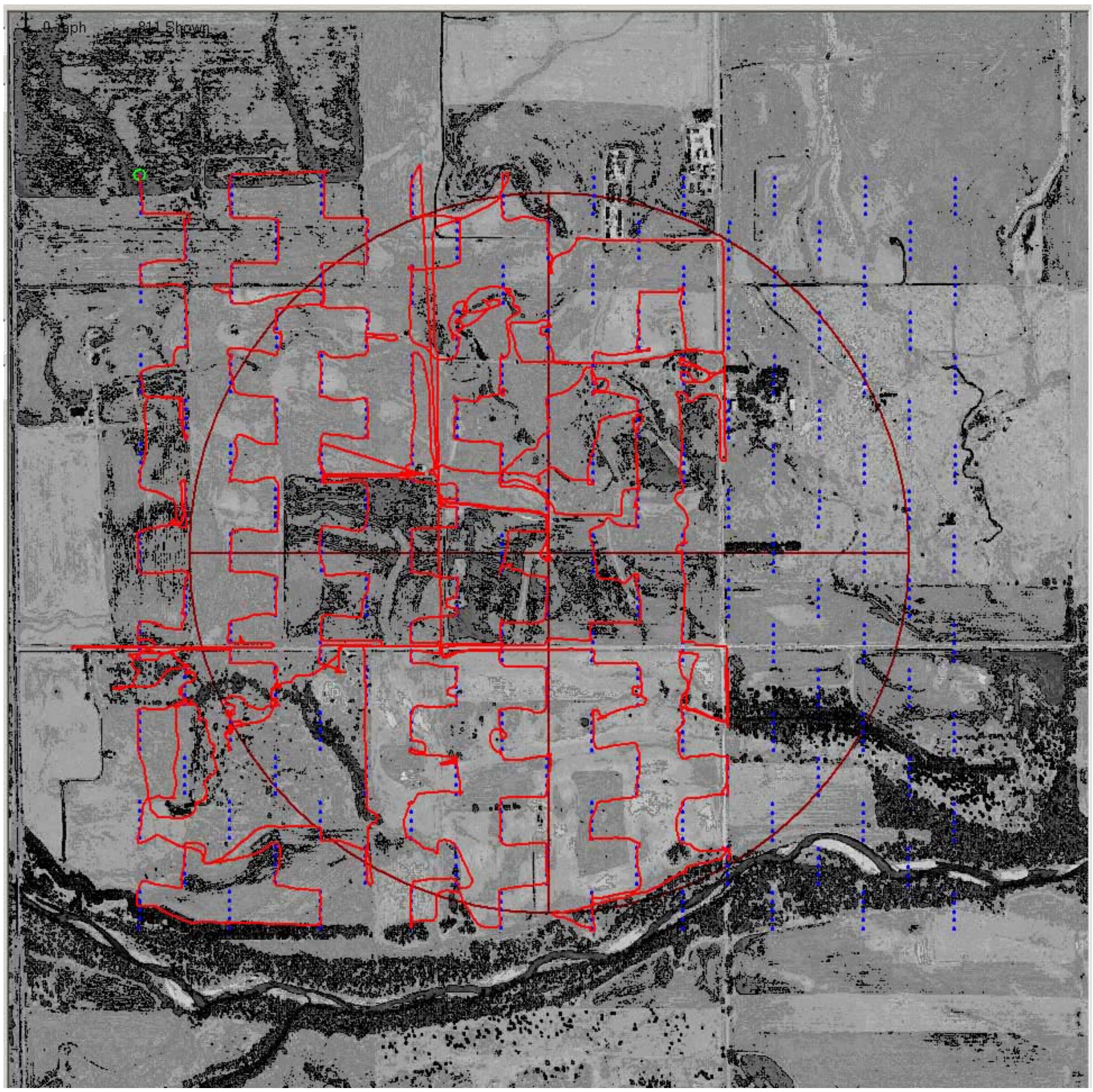

Figure 4. An orthophoto of the project area overlain by a preliminary tracking log.

After three site visits and extensive route mapping (necessary for computer-aided guidance system on vibrator), areas in need of line clearing were identified and permission to clear granted from the affected landowners/tenants. To insure the optimum trace configurations (azimuthal, offset, and fold symmetry) and year-to-year and season-to-season consistency in source locations over the six years of this monitoring program, source access paths were made as straight as possible and clear of overhanging trees that might interfere with satellite reception (Figure 5). To minimize the impact on the vegetation and to maximize the consistency in source and receiver coupling, paths were made narrow with as many of the large relief river terrace features cut and smoothed (in some cases as much as a meter) to reduce the potential static anomalies and to allow all-season travel along the paths.

A dozer, tracked hoe, and several trucks were used to clear the paths (Figure 5). Several of the source lines in the extreme southwestern end of the patch ended right at the Smoky Hill River. Cuts up to 1 m were made through the steeper terraces, cutting away the loose sandy near-surface to expose a more compacted surface, a significant improvement in the coupling environment for the vibrator. To move the source through these areas, some manicuring was necessary and the more extreme slopes cut down. In most places the ground was just scraped, with the larger trees directly in the source line removed, leaving a path that was around 12 to 15 ft wide. The old gravel pit had several

Figure 5.

old mined-out ponds and channels that left a hummocky topography. With a few exceptions, the source paths are straight north/south.

**Seismic Data Acquisition: Baseline Survey**

Acquisition of the baseline 3-D survey for the 4-D seismic monitoring project began on November 5, 2003. Digital data from preliminary GPS surveys were used to guide physical site preparations and were integral to the construction of an extremely accurate and precise station grid map. The station grid map incorporated the 3-D seismic survey designs with the site-specific information and allowances for surface obstacles. Ensuring the placement precision of this and all repeat source and receiver line deployments is critical to difference processing. Digital terrain maps with vibrator routes were built for all 800+ source locations across the site. Considering the six-year duration of this surface seismic monitoring project, time spent at this stage to accurately map each detail of the data acquisition phase helped ensure maximum correlations between repeat surveys and minimized the need for radical equalization procedures during data processing.

Figure 6.

Figure 7.

Each receiver line was located with a Trimble DGPS to ensure straight grid lines (Figure 6), with deviations in line-to-line spacing not exceeding a couple percent (1 m to 2 m). Three Mark Products U2 10 Hz geophones with 14 cm spikes were placed at the points of a half-meter equilateral triangle centered on the receiver station. With the receiver grid remaining on the ground for up to two weeks, the geophone connections were protected from moisture and ground leakage by suspending them in the air with plastic bowls (Figure 7). This practice reduced and generally eliminated all earth signal leakage. Each receiver was planted at the base of a hole dug down through the sod and into firm soil (Figure 8). This ensured good coupling and reduced the effects of wind noise.

Figure 8. (left and right)

A Geometrics NZ StrataVisor was used to record data from a 24-bit A/D, 241-channel Geode distributed seismograph system. Each Geode (11 individual units) contains 24 recording channels and is connected to the StrataVisor (controller) through reinforced Ethernet cables. The StrataVisor remotely controls the entire acquisition process and provides a variety of QC functions to ensure data quality. Interfaced to the StrataVisor was an IVI RTS (radio control unit for communicating with the vibrator and receiving the sweep from the vibrator) delivering the ground force pilot to the StrataVisor where it was recorded on an auxiliary channel. Two 24-channel Geodes were deployed in the center of each receiver line (Figure 9 left). These distributed seismographs transmitted digital data through four unique Ethernet lines daisy chained between units located at the center of each of the five receiver lines. An 85-amp-hour deep-cycle marine 12-volt battery powered two units for more than 40 hours of continuous use. The four Ethernet lines were all connected to the NZC controller located centrally within the receiver patch (Figure 9 right). Warm and clear weather conditions allowed open-air operation of the seismic controller. Temperatures ranged from lows of 60ºF to highs near 90ºF.

Data were recorded uncorrelated, allowing maximum flexibility during processing to enhance the high fidelity of the data through precorrelation processing and unconventional approaches to correlation. Each sweep was recorded as a separate file, resulting in more than 4,000 files and a total of about 12 megabytes of data per survey. A single 3-D survey consumed about 40 gigabytes of storage space. The recording system was housed on the back of a specially modified John Deere Gator 6-wheel vehicle (Figures 10 and 11). Due to the need for quiet operation, six 12-volt lead acid batteries provided all power. Temperatures below freezing required housing the operator and system inside a specially designed insulated covering previously used during KGS research north of the Arctic Circle (Figure 12).

Figure 9. One of five Geode deployments (left) located in the center of each 48-station receiver line. The five Geode groupings were all connected to the Geometrics StrataVisor NZC seismic controller (right). Conducted from this John Deere Gator, seismic operations were all-weather and all-terrain. Here the Gator is configured for warm, dry conditions. Under wet or cold conditions an additional zip-on covering can be added to protect the operator and seismographs.

Figure 10.

Figure 11.

Figure 12.

Figure 13.

A differential GPS transmitter was set up directly over the $CO_2$ injection well and used for vibrator guidance, receiver placement, and well locations (Figure 13). The transmitter was up and operational during this entire baseline survey and will be used on all future surveys to ensure all source locations are within 0.5 m of this baseline survey and receivers are placed within centimeters of their current locations.

Capabilities for night operations were essential to avoid cultural and wind noise, which would severely contaminate this low-energy high-frequency data. To ensure safe and accurate movement and placement of the vibrator, a GPS guidance system specially designed at the KGS for this project was installed on the vibrator (Figure 14). The system allowed navigation around the site and to each shot location along predetermined optimum paths. From the cab of the vibrator the operator could move repeatedly along these predetermined routes within a few inches of the programmed safest route to a shot location, all in total darkness, if necessary. Once the vibrator was located and a sweep run, the onboard computer would log the exact pad location (within a few inches in x, y, and z).

Figure 14.

Considering the study area for the 4-D seismic survey was just over one square mile, the diversity in terrain was significant and provided unique challenges (Figures 15-19). Source as well as receiver coupling was critical, and for that reason five individual sweeps were recorded at each location. Each of the 10-second linear up-sweeps spanned the 20 Hz to 250 Hz frequency range in a temporally uniform fashion. The first of the five sweeps was designed to seat the pad (compact the ground sufficiently that subsequent sweeps are as consistent as possible) while the remaining four sweeps were vertically stacked (once appropriate noise was edited from each) to enhance the signal-to-noise ratio. Areas such as freshly planted wheat fields were the softest and were the least conductive of high-frequency signal. Other areas such as pastures, roads, summer-fallowed ground, waterways, alfalfa fields, and wooded areas all affected vibrator performance in slightly different ways. Of particular concern was maintaining source locations that would not only be accessible for the six-year duration of this study but also minimize dramatic swings in ground conditions due to seasonal changes. Dealing with this variability in source and receiver coupling was best accomplished during the recording phase rather than relying on processing to numerically compensate for these effects.

Figure 15.

Figure 16.

Figure 17.

Figure 18.

Figure 19.

To insure acquisition of the highest quality data set, all shot records were re-viewed and preliminary processing completed on each vibrator sweep on-site (Figure 20 left). With the over 4000 uncorrelated, 12-second vibrator sweeps recorded as part of each 3-D survey, real time on-site QC was essential. Uncorrelated shot records were downloaded via Ethernet to on-site computers located in the mobile processing center (MPC) (Figure 20 right). Then the data were corrected for spectral attenuation, correlated, spectral balanced, edited, filtered, and vertically stacked. Data from shot stations with excessive noise or noise inconsistent with that observed on records from other shot stations in proximity were re-recorded to improve signal quality.

Figure 20. View from front of truck toward computer workstations (left); processing box (right) is climate controlled and mounted on truck frame with ride-controlled air suspension. A 12-kilowatt generator provides both 240-volt and 120-volt power. As data were acquired they were transmitted via Ethernet from the seismograph to the mobile processing center. Once data were transferred, preliminary processing was

performed, which included long-term archive, format conversion, pre-correlation processing, correlation, noise editing, vertical stacking, application of geometry, and data inspection.

During data inspection and preliminary analysis, stations that needed reoccupation and reacquisition of data were defined. Ability to identify poor data areas and redeploy the source to these areas within hours of acquisition was only possible as a result of this in-field processing capability. About 15 percent of the shot locations were reoccupied in an attempt to improve data quality. This clearly enhanced the uniformity of the fold and resulted in a final data set with 3-D acquisition characteristics (fold, azimuthal and offset distribution, etc.) that more closely matched the ideal design criteria.

**Seismic Data Acquisition: Monitor Survey One**

Deployment of recording equipment for the first 3-D monitoring survey began on January 17, 2004, approximately six weeks after the baseline 3-D survey and start of $CO_2$ injection at the 10-acre enhanced oil recovery (EOR) demonstration site in southeastern Russell County, Kansas (Figure 21). Based on rough reservoir model estimations and the assumption $CO_2$ is moving uniformly away (horizontally) from the injection well, the $CO_2$ front should be at least 75 m, roughly seven bins or subsurface seismic sample points, out from the injection well.

Figure 21. Kevin Axelson, Foreman for Murfin Drilling Company, monitors $CO_2$ pressure.

In November 2003, just prior to initiation of the $CO_2$ injection, a 3-D baseline survey of over 800 shot stations was conducted (Figure 22). High-resolution GPS was used to navigate the site and insured each source location would be reoccupied within 0.5 m on all subsequent acquisition trips. Besides navigation, the DGPS system was programmed to provide a digital terrain map with an overall accuracy of better than 0.5 cm for each occupation point (Figure 23). Baseline reflection data were acquired intermittently over five days with stoppages for excessive wind, construction around the tank battery, and activity associated with well rework rigs. Night recording proved beneficial in minimizing wind and cultural noise.

Figure 22. Vibrator tracking log showing all source stations occupied and routes driven.

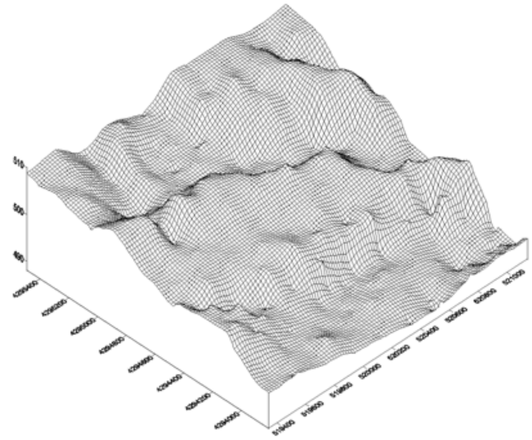

Figure 23. Digital terrain map from vibrator.

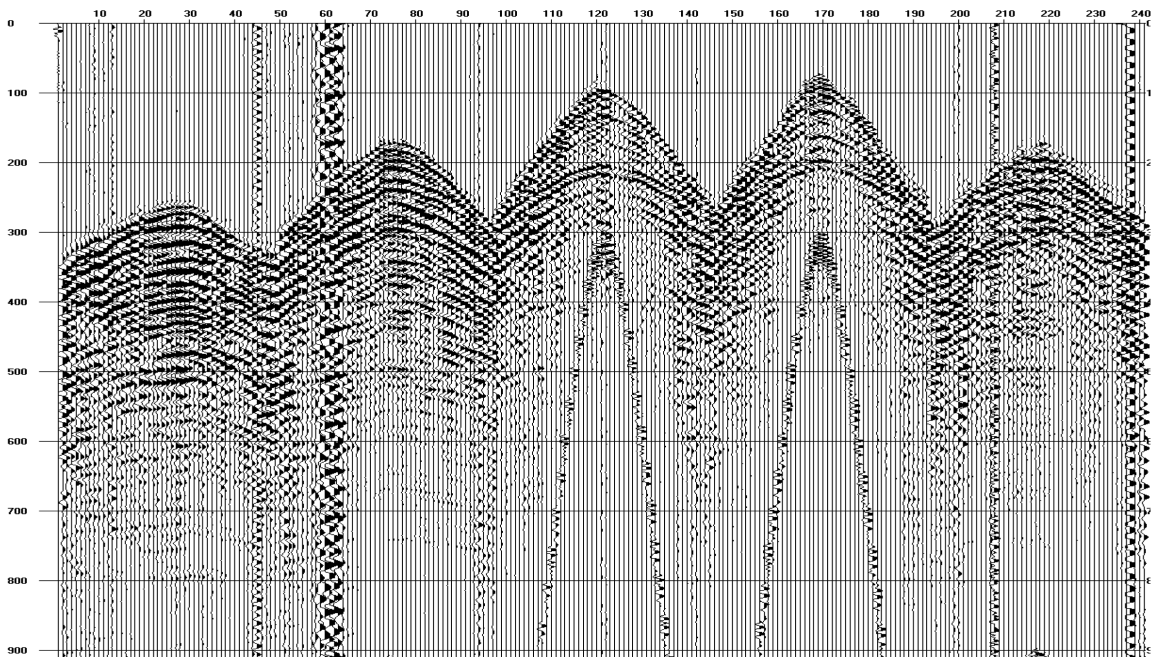

Figure 24. Correlated shot gather from station 19047, near center of receiver spread.

Data quality from the baseline survey was excellent (Figure 24). Data were cross-correlated with the synthetic pilot trace after whole trace gain was applied, boosting the amplitude of the high frequency signal (1 second AGC scale). After correlation, coherent noise with an arrival pattern that changed from sweep-to-sweep (vehicles) was removed by zeroing affected portions of the data. Once the signal-to-noise ratio was maximized on each correlated sweep, the last four sweeps (five sweeps were recorded at each site, but the first sweep was only used to seat the base plate) were then vertically stacked.

A total of almost 800 240-channel shot gathers were recorded for each survey. Each shot gather is a four-shot vertical stack. With simple spectral balancing (band-limited spiking deconvolution) the dominant frequency of the reflection increased from around 70 Hz to over 100 Hz, which equates to an improvement in resolution potential from 35 ft to around 25 ft at depths in excess of 3000 ft (600 msec) (Figure 25). As the data processing continues, the dominant frequency from 3000 ft could exceed 150 Hz, thereby providing vertical resolution potential of around 15 ft with an upper usable corner frequency of over 200 Hz, making the thinnest possible bed resolution at around 12 ft within the Lansing-Kansas City (L-KC) formation. Approximate two-way travel time of the interval of interest (L-KC) using NMO calculated average velocities is 600 ms. Several high quality reflections are evident between 500 and 800 msec. The top of the Arbuckle is likely the reflection at around 750 msec at longer offset traces with basement around 800 msec (Figure 25). Processing of the 3-D baseline data set into a stacked volume was completed by mid-February 2004.

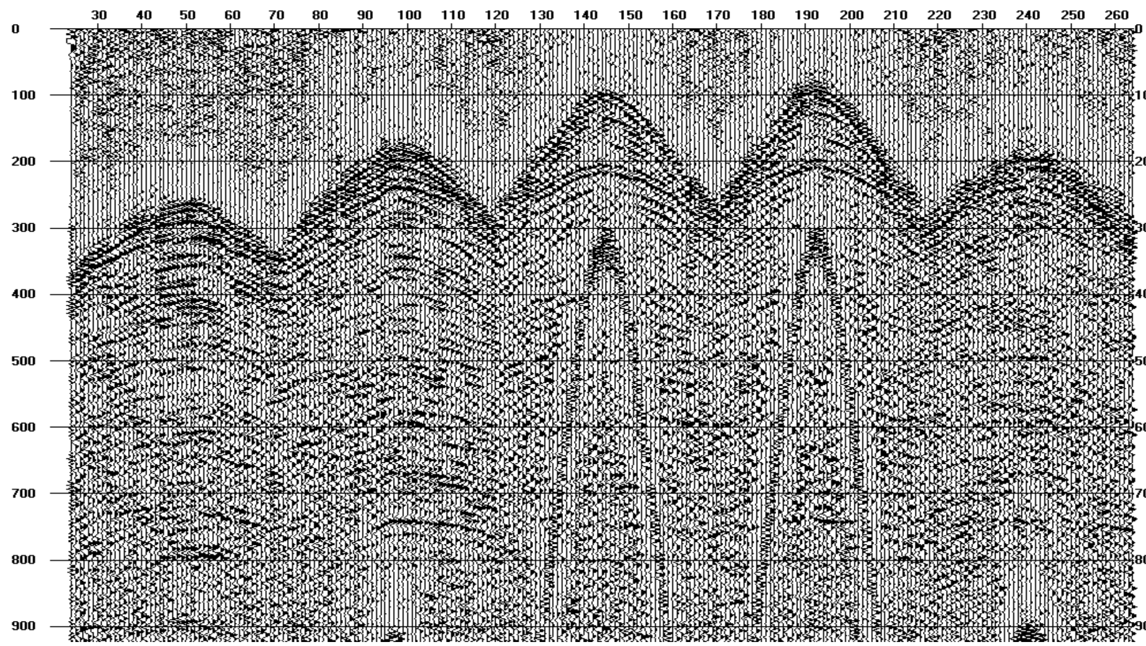

Figure 25. Four-shot vertical stack with spectral balancing.

Without doubt equipment upgrades and prototype components used to acquire these 3-D data more than doubled the overall signal-to-noise ratio and noticeably boosted the dominant frequency (Figure 26). Walkaway tests acquired during August 2002, using a 240-channel Geometrics Strataview seismograph (21-bit A/D) and IVI minivib1 (1500 ft-lbs @ 200 Hz) with the standard factory valve, produced data with excellent potential and quite adequate for the proposed 4-D monitoring project (Figure 26). However, upgrading the seismograph from 21 to 24 bits of dynamic range (going from a Geometrics StrataView to a distributed Geometrics Geode system) and quadrupling the power output of the vibrator by going to a minivib2 with a high output Atlas rotary valve dramatically elevated the potential effectiveness of this technique to monitor, track, and allow prediction of $CO_2$ movement with little increase in overall cost.

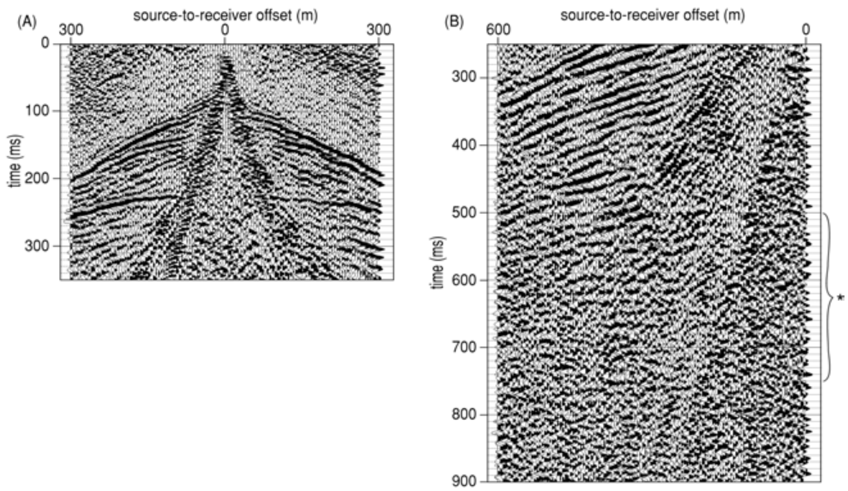

Figure 26. 2-D shot gather acquired during August 2002 testing with the minivib1 and Strataviews.

Equipment was transported to the field site in two semi-trailers (Figure 27). One hauled cables, phones, and vibrator (Figure 27 left), while the other transported the ATVs used to haul cables and phones and house the recording equipment (Figure 27 right). The semi-tractor used to move the ATVs and seismograph to the site also houses the mobile processing facility (MPC), which contains three workstations, two printers/plotters, and enough desk space for three processors (Figure 27 right). All on-board computers are connected to each other and the seismograph via Ethernet cables.


Figure 27. Two semi-trailers transport equipment to the field: (left) cables, phones, and vibrator, and (right) ATVs and seismograph.

Time-lapse analysis of these two data sets (baseline and the first of eleven 3-D monitoring surveys) required minimal, if any, special equalization procedures to compensate for changes in ground or recording conditions. Data acquisition on the first monitoring survey mimicked the baseline survey as closely as possible. Ground conditions across the site were nearly identical to what they were in November just two months prior (Figure 28). With no appreciable new moisture and with ground conditions that were already extremely dry, from a seismic data perspective surface or near-surface conditions were unchanged between this survey and the baseline 3-D survey collected six weeks prior.

Figure 28. Ground condition on January 17. Air temperature was 40° F & wind at 25 mph.

Cables were laid along receiver stakes placed during baseline survey (Figure 29 left). Geophones were planted in the same locations (+/-10 cm) and with nearly identical coupling (Figure 29 right). To insure as near identical recording conditions as possible, no data were recorded when wind speeds are in excess of 15 mph, with reluctance to record when the wind exceeds 10 mph. These general ground rules for recording in this notoriously windy area were used during the baseline survey and will be used for all 3-D monitoring surveys.

Figure 29. (left) cable laid with ATV along stakes and (right) geophones planted at surveyed stake.


Figure 30. During normal operations $CO_2$ will occasionally vent from storage tanks.

With time lapse (4-D) seismic imaging comes an exorbitant amount of attention paid to all sources of noise, especially noise that changes from record-to-record and day-to-day (Figure 30). This concern stems from the need for complete repeatability in every recorded data point. Sources of noise at the $CO_2$ pilot study site in southeastern Russell County include wind, rain/sleet, injector pumps, injection wells, pipelines, oil-production pumps, vehicle traffic, livestock/wildlife, and power lines. Each of these noise sources produces seismic energy impacting the recorded signal in a range of ways.

Changes in near-surface conditions that occurred during the acquisition of the first 3-D monitoring survey (January 20 to January 30) had little to no effect on the recorded data (Figure 31). Receivers were well seated (14 cm) into solid material and all electronic connecting points were insulated from the ground by elevating the takeouts with plastic tubs and therefore protecting the takeout from leakage (Figure 32). The 240-channel Geometrics Geode recording system is designed to operate in all weather conditions (Figure 33). When noise from sleet hitting the receivers was observed, recording was halted until the sleet stopped.


Figure 31. Data collection: Jan. 23 (50º, calm, & clear) vs. Jan. 25 (25º, freezing rain, and cloudy).

Figure 32. Ten-hertz geophones with tubs to insulate connector.


Figure 33. Ice covered Geode.

Coherent noise that moves either during the 10-second seismic sweep or from sweep to sweep at a single source station has the least impact on the eventual consistency in data characteristics between any two surveys acquired at different times of the year. Moving coherent noise is generally a vehicle, an animal, or humans. Since the source point for this type of noise changes from shot to shot throughout the recording time, it can be muted or zeroed from one record in a surgical fashion (Figure 34). In this example, when the four sweeps from each station are vertically stacked, contributions from records with good signal are added to the zeroed or muted portions of records where noise had previously dominated to produce a continuous high signal-to-noise ratio section.

Removing coherent noise that is stationary is more difficult than moving coherent noise. Examples of sources of coherent stationary noise include injection wells, injection pumps, pipelines, oil-production pumps, and power lines (Figure 35). With the stationary nature of these noise sources, all records recorded for all source locations had this noise at the same place (Figure 36). Therefore the method used for moving noise sources—muting bad segments and then adding the muted (zeroed) portion to good signal from other records taken at this site—will not work here. Two different techniques were used to reduce or eliminate this type of noise, depending on the specific characteristics of the noise. One technique involved filtering in the frequency domain for the noise source, which has dominant frequency signatures within a narrow range or a range outside the seismic source bandwidth. Another technique is cancellation when the phase characteristics of the noise source vary through time and from record to record.

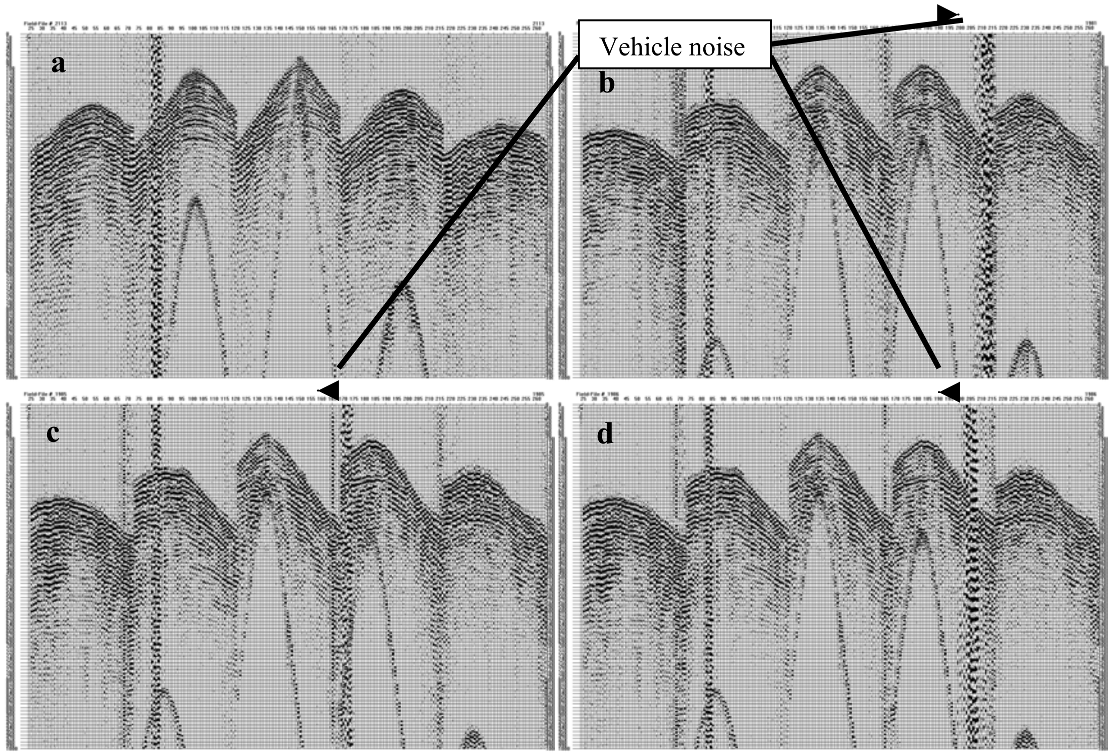


Figure 34. (a) Quiet record with water injector pump at trace #84, compared to records (b), (c), and (d) with vehicle noise moving across the records.

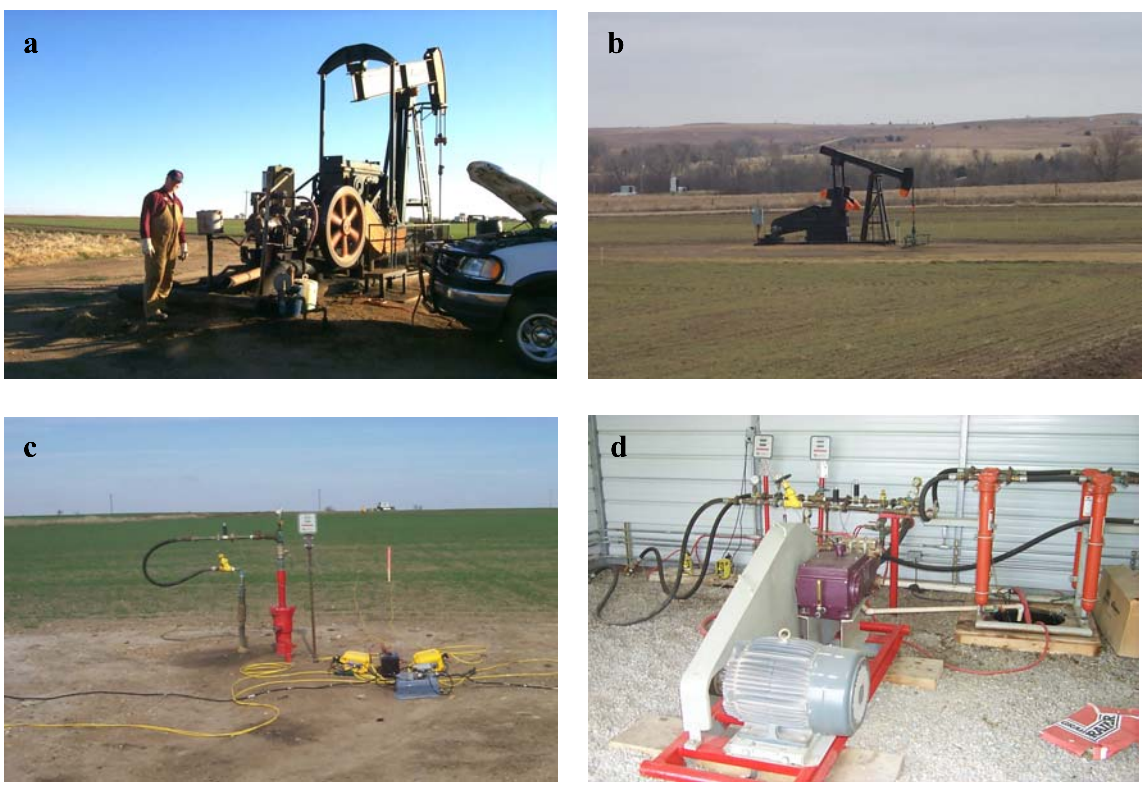


Figure 35. (a) Single cylinder gas engine powered pump jack, (b) electric-powered pump jack—Colliver #12, (c) water injection well with fluid flow meter, (d) piston pump for water injection.

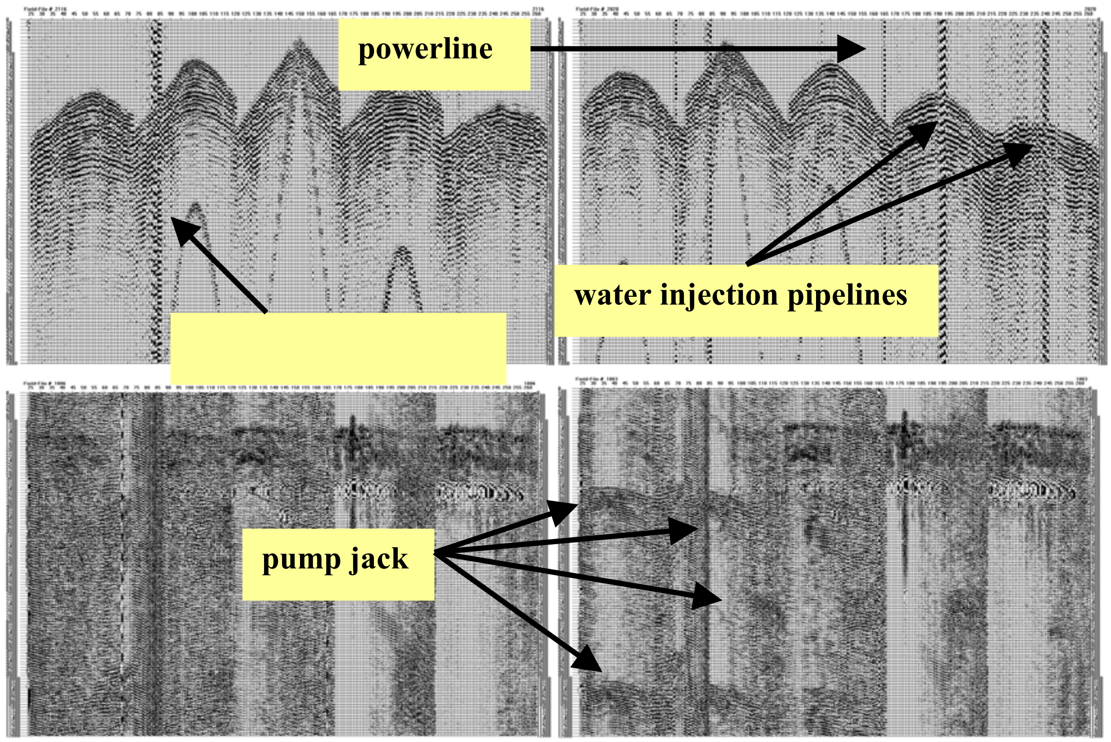

Figure 36. (top) Correlated shot gather with stationary noise. (bottom) 12-second uncorrelated shot gather with pump-jack noise (right) and without (left).

At this site there are two predominant sources of fixed, continuous, coherent noise: pumps and pipelines. Oil-production well pumps produce a periodic low-frequency long-duration pulse consistent with the stroke of the pump jack (Figure 35). Correlation of the pilot with the recorded sweep tends to reduce this kind of noise, generally to levels that can be tolerated, but not preferred, on 4-D data sets. This kind of pump jack noise is bothersome but not nearly as detrimental to the overall data quality as ground vibrations emitted by high-pressure piston pumps. High-pressure piston pumps put continuous high amplitude relatively broadband noise into the ground.

In the case of the fresh-water injection pump located inside the utility shed on-site, all receivers within 150 ft are inundated with this high amplitude broadband noise (Figure 36, top). The only signal enhancement weapons that seem to work to a very limited degree against this kind of noise are spectral balancing and vertical stacking. Fortunately, these pumps do not saturate the available dynamic range of the seismograph, permitting recording of some signal (be it extremely low amplitude). This extremely small percentage of signal increases relative to the noise by vertically stacking each sweep recorded at a shot station. Building the signal strength in this fashion is possible as a consequence of the uniformity in arrival times and character of signal on all shot gathers compared to the more random phase-time relationship that coherent and continuous single-point noise will have from shot to shot.

Pipelines used to move the fluid from pump to well bore emit noise generated by surface piston pumps, which are used to move fluid around an oil field (Figure 36, top).

A tremendous amplitude of pump noise can be seen every place a pipeline passes beneath a receiver line. With water injection at this site used to contain the $CO_2$, pumping of water through these pipes and into the injection wells occurs based on need as determined by borehole pressures. Therefore, high-amplitude pipeline noise dominates several traces on any line that passes over the pipeline for periods of 1 to 2 hours every 2 to 4 hours all day. This noise always affects the same receivers but is recorded at some shot stations and not at others, depending on when the well pressure dictates. As a result, no two complete 3-D data sets will have this pipeline noise on all the same shot gathers. Differences in this noise will show up as a change from baseline to later monitoring surveys.

Wind is a source of noise that is the least controllable and can be the most detrimental to time-lapse seismic recording (Figure 37). No two days have the same wind conditions, so it is impossible to record two data sets that will difference to equal zero even when using the same source, identical source locations, and exactly the same receiver grid. This project requires four to six days to record data from all the source locations. Across that six-day span, noise from wind is stronger some days than others, making shots recorded from one side of the grid noisier than shots from the other side, regardless of near-surface conditions or source-to-receiver offsets. On this project, no data are recorded when wind velocity exceeds 15 mph. This is an experience-based value that resulted in an acceptable signal-to-noise ratio on recorded seismic data.

Figure 37. Data acquisition was not possible on Jan. 26 (10º F, snowing, and 30 mph wind).

Figure 38. (a & b) Conditions during week of January 19; (c & d) conditions during week of January 26.

Adjustments made to the data-acquisition procedures insured changes from the dry, warm conditions present at the start of this survey to the snow/ice covered ground and frigid temperatures endured during the latter days of this first 3-D monitoring survey (Figure 38) had little or no distinguishable effects on the recorded data. For example, the vibrator pad was continuously cleared of snow to maintain optimum coupling. KGS experience acquiring data in Arctic regions was extremely beneficial in and critical to maintaining the highest possible data quality even when temperatures dropped below -6ºF with a stout breeze and light snow cover on the ground.

Qualitative analysis was used to determine if shot records possessed unacceptable noise levels. Determining stations that needed to be reoccupied was generally a straight-forward process. High frequency random noise, elevated by as much as 6 dB over adjacent stations, could be easily identified. In general, noise level increases of as little as 3 dB were sufficient to justify reacquiring all five sweeps at that location (Figure 39).

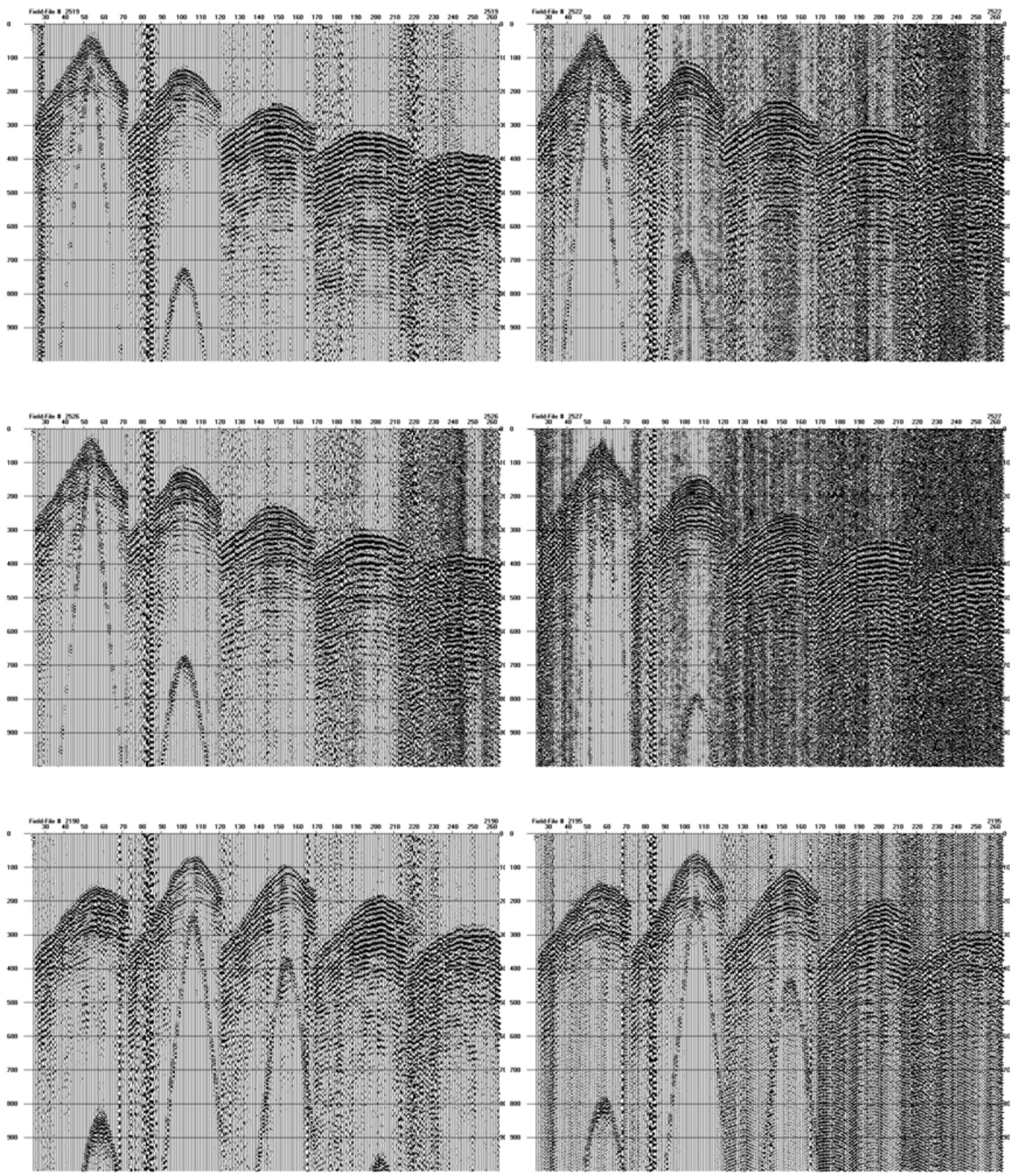

Figure 39. Average, relatively low noise, correlated shot gather (left) with adjacent shot station (right) possessing elevated noise levels.

Visually dramatic increases in noise between two source stations located within 20 m of each other are usually related to earth coupling of the vibrator or gusty winds. Either way, reacquiring the data can only be accomplished real-time while all the equipment and crew are on-site and the $CO_2$ position is relatively constant (at least with respect to the size of the seismic wavelet). Considering the need that time-lapse analysis has for high S/N data, this step is imperative for obtaining the highest resolution, most representtative series of snap shots of the $CO_2$ movement through this shallow (950 m), thin (5 m) reservoir.

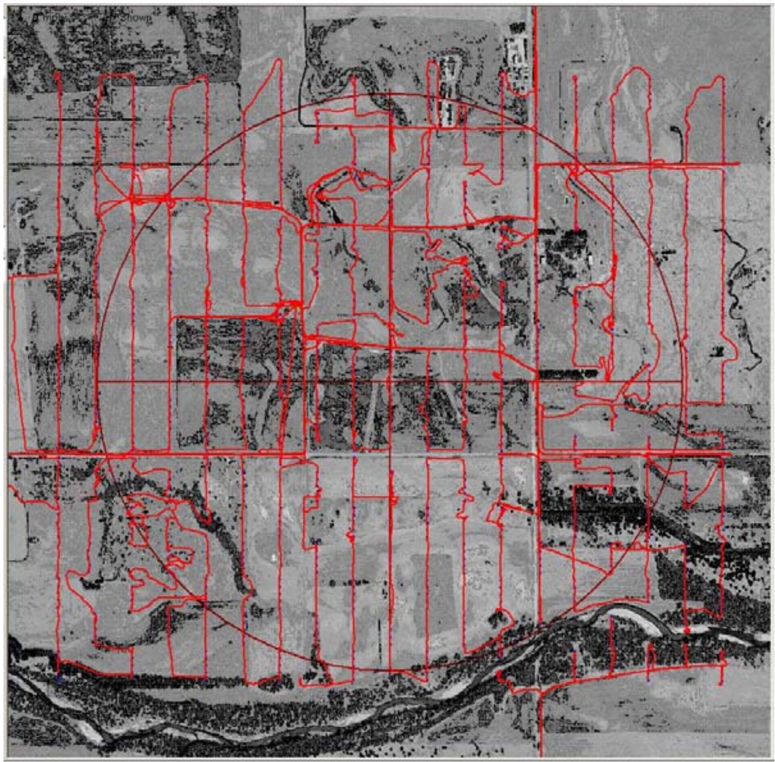

Figure 40. Vibrator tracking log from the January 3-D data acquisition trip (first monitor survey). Red lines are the continuous (1/second) DGPS readings on the vibrator's location. The orthophoto in the background provides some insight into the surface conditions and morphology. A total of 795 points were occupied during this survey.

**Seismic Data Acquistion: Monitor Survey Two**

Incorporating all currently available well data, engineers projected $CO_2$ breakthrough in Colliver 12 as early as April 1, significantly ahead of preliminary schedules. Predictions of premature breakthrough at this oil-producing well were revised based on models that incorporated wellhead data acquired during water-injection tests run just months before commencing the $CO_2$ flood. These newer models suggested movement along the $CO_2$ front was being influenced by high-permeability "fingers." These high-perm zones influence connectivity between Colliver 12, 14, and CO2I#1 and are likely quite thin (on the order of a seismic wavelength). It was anticipated from seismic-waveform models produced from pressure and phase relationships that as the $CO_2$ front passed the amplitude of the reflectivity of L-KC, the C-zone reflector would change sufficiently to allow easy tracking of the $CO_2$ plume from comparison of images from the first two 3-D seismic surveys.

After deliberation among geologists, engineers, and geophysicists, the optimum second snapshot of the $CO_2$ flood-monitoring survey (third 3-D survey; one baseline and two monitoring) needed to begin around March 15 (Figure 41). Based on previous experience, this third 3-D survey was expected to take about 10 days. Geophones were left frozen in place after the January 2004 survey and were used for this survey without disturbing them (Figure 42). Considering the effort taken between surveys to reoccupy identical stations and plant geophones well into competent soil, leaving the receivers in place did not result in distinguishable changes in survey-to-survey consistency.

However, this difference was studied and if significant improvement in waveform consistency would have been observed receivers would have been left in the ground where possible, although tillage of farm fields would not have permitted phones to remain planted in some areas of the site.

Figure 41. Installing cable protector across road.

Figure 42. Connecting geophones still in place after January 2004 survey to cable laid down for March 2004 survey.

Critical to data quality during the second monitoring survey at the $CO_2$ injection site was the avoidance of excessive wind noise. March is known as particularly windy in central and western Kansas. Noise from wind is difficult to attenuate using post-acquisition processing techniques on seismic data due to its somewhat random arrival pattern and broadband spectral characteristics. Major efforts were taken to minimize the recording of excessive wind noise. Most significant of these efforts were recording at night and only recording when winds were less than 15 mph (an empirically based wind speed based on noise levels observed at the seismograph during recording). As a result of these strict acquisition guidelines, several days might pass without data being recorded while other days more than 240 shotpoints were recorded in a twenty-hour work period.

With temperatures in the 60s, ground surface dry, and winds less than 15 mph, background noise levels and site access conditions were as close to ideal for this part of the world as possible for seismic-data acquisition during March. When the wind exceeded 15 mph, the data quality dropped sufficiently that acquisition was halted (Figure 43). Generally, during the afternoons wind velocities exceeded acceptable levels for recording. To counter these unacceptable noise levels, data acquisition began around 3:00 am and continued until wind levels exceeded preset thresholds, usually occurring around 12:30 pm to 1:00 pm (Figures 43 and 44). The requirement for low wind noise is significantly more important for 4-D (time-lapse) than for standard 3-D. For 4-D to be effective, detectable changes in reflection signatures must primarily be related to changes in reservoir flood properties and not due to changes in noise levels or ground conditions.


Figure 43. Wind gusting at 30 mph in afternoons.


Figure 44. No wind, night and mornings.

Wind noise became a noticeable problem when gusts exceeded 15 mph. Shot records from the end of the first day showed the adverse affects of winds gusting to around 20 mph around 1:00 pm (Figure 45). Reacquiring noisy data from day 1 just 14 hours later on day 2 when winds were calm resulted in a noticeable improvement in the signal-to-noise ratio (Figure 46). A great deal of on-site effort went into identifying shot records possessing unacceptable noise levels and reacquiring those stations when conditions were more conducive to the highest quality data possible.

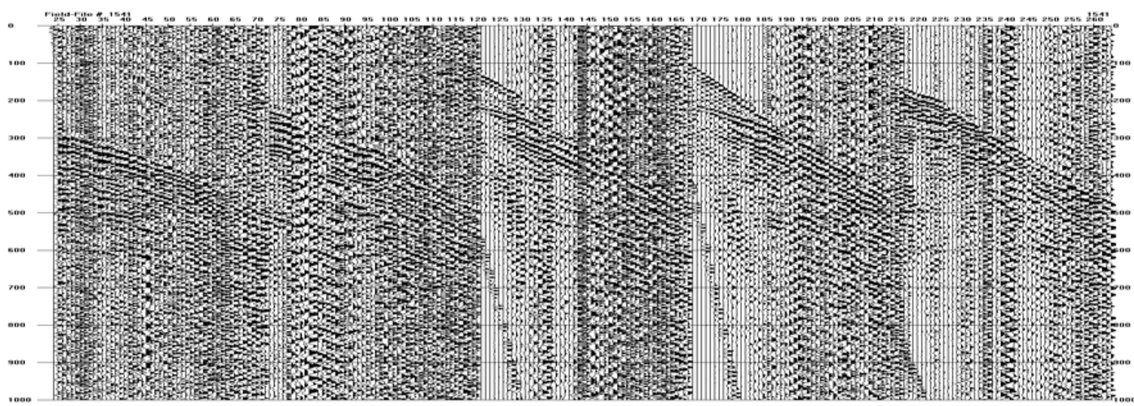
Figure 45. Correlated single sweep from station 13049 with 20 mph gusty winds.

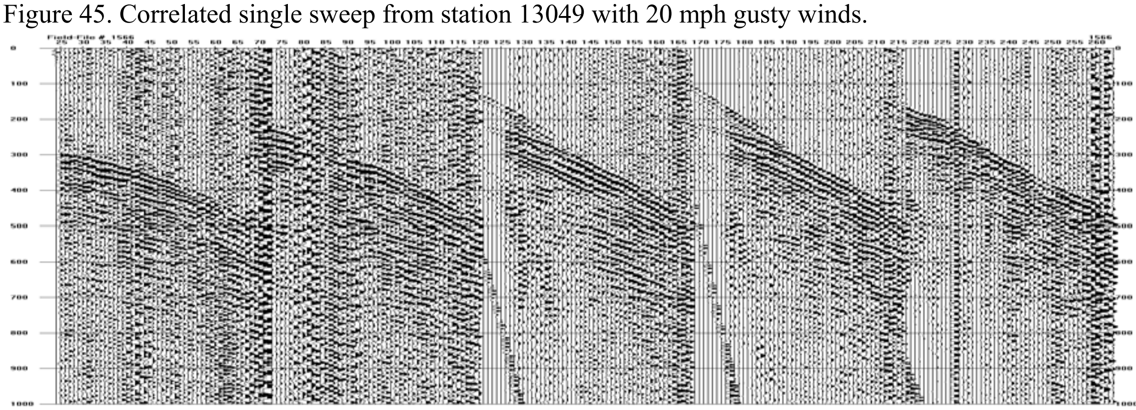
Figure 46. Correlated single sweep from station 13049 with no wind.

Shot gathers from the first three surveys, in general, were of very good quality (Figure 47). Repeatability of reflection amplitudes and source-wavelet characteristics was better than expected and clearly demonstrated the advantages of consistency in all aspects of the data acquisition on time lapse. This repeatability greatly reduced the importance of computational-equalization techniques that have been essential to time-lapse analysis on most other 4-D seismic surveys. Coherent energy arrivals with hyperbolic moveout, characteristic of reflections, were interpretable throughout the primary depth interval. More than a dozen individual reflections returning from between the Stone Corral Formation and Arbuckle were easily identifiable on the shot gathers with guidance from the downhole survey acquired in #16, the synthetic seismogram, and published data from this general area.

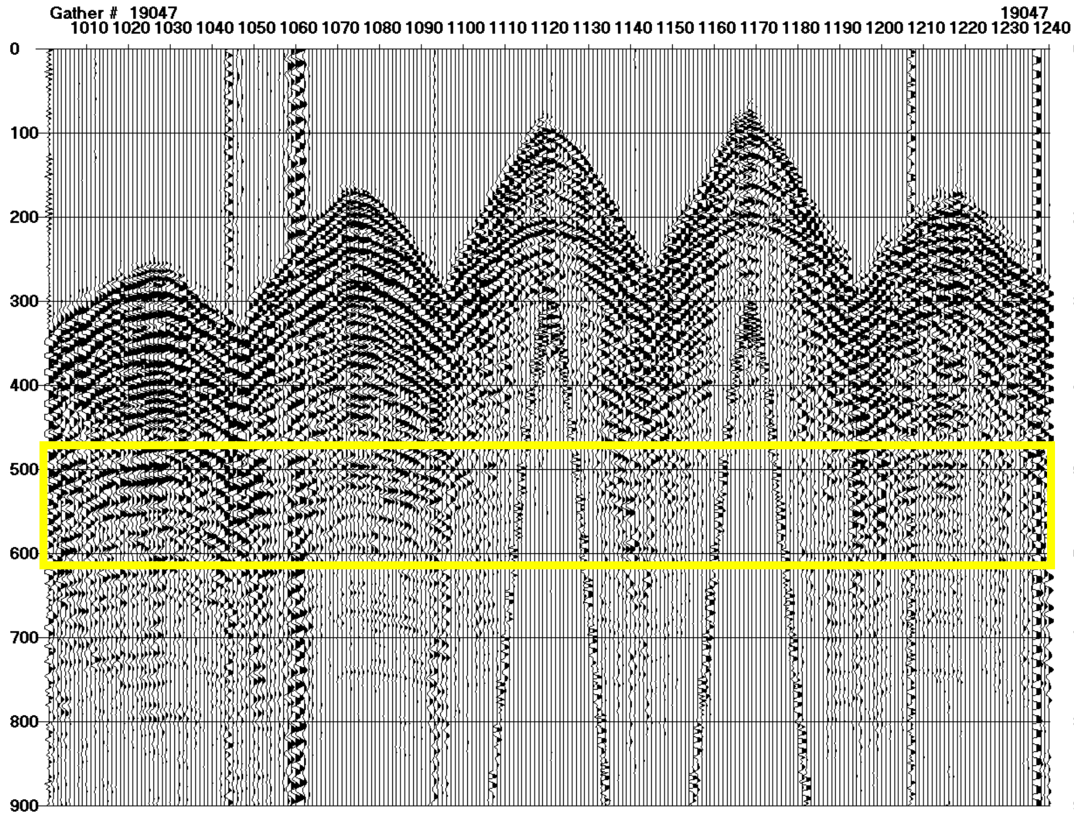
Gather # 19047
19047
1010 1020 1030 1040 1050 1060 1070 1080 1090 1100 1110 1120 1130 1140 1150 1160 1170 1180 1190 1200 1210 1220 1230 1240
0
100
200
300
400
500
600
700
800
900

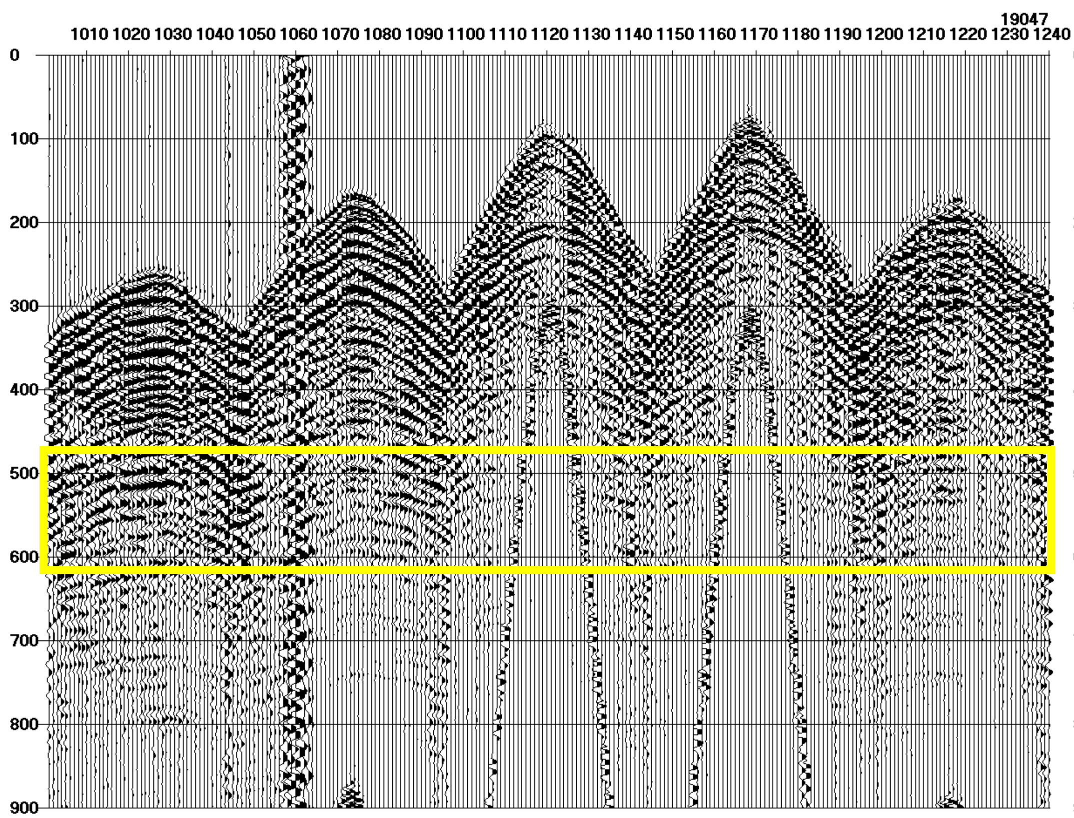
19047
1010 1020 1030 1040 1050 1060 1070 1080 1090 1100 1110 1120 1130 1140 1150 1160 1170 1180 1190 1200 1210 1220 1230 1240
0
100
200
300
400
500
600
700
800
900

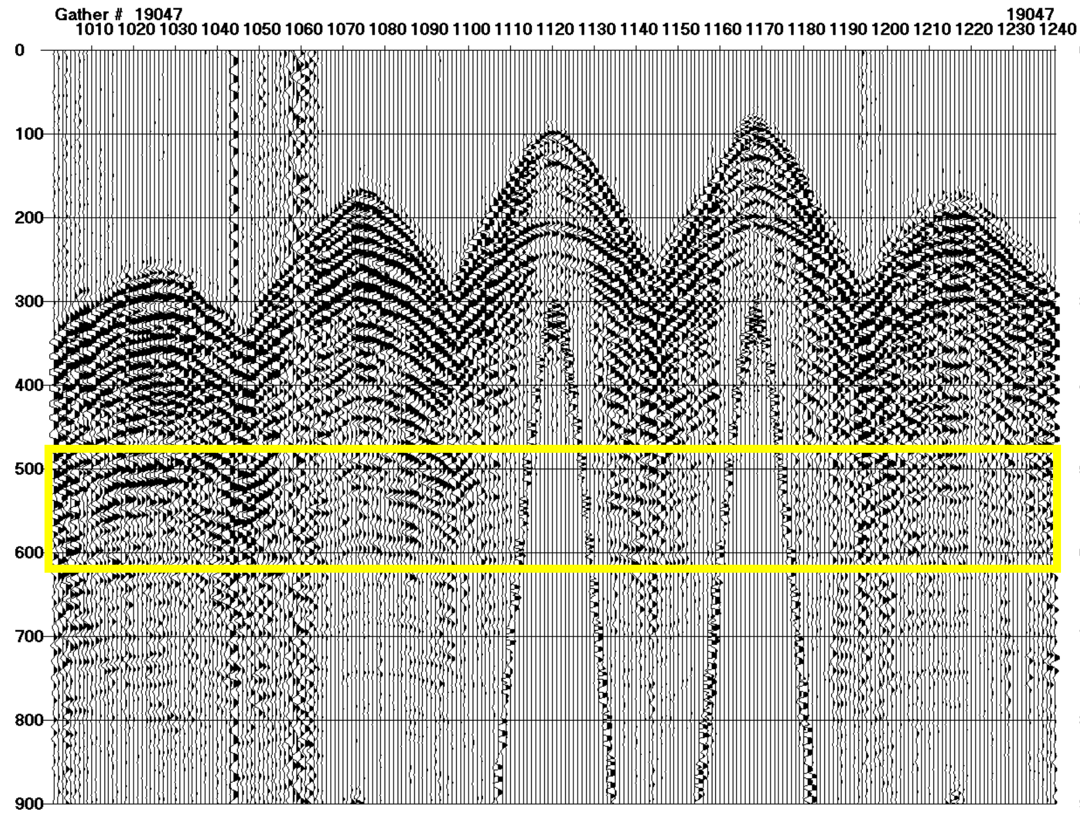


Figure 47. Comparison of shot gathers from three trips. Before $CO_2$ injection (top), after six weeks of $CO_2$ injection (middle, ~200,000 gallons), and then after slightly than three months of $CO_2$ injection (bottom, ~450,000 gallons). Reflections from the Lansing-Kansas City (L-KC) should be arriving between 550 and 590 msec, depending on source offset. Exact time depths are determined from VSP and synthetic seismograms produced from nearby sonic logs. The boxed area is enlarged in Figure 48.

Meaningful correlation of the synthetic traces with traces from a shot gather requires estimates of reflection-arrival time based on source-to-receiver offset, time shifts that are compensated for on vertical incidence, and CMP-stacked sections using the NMO correction. Based on reflection-curve modeling, reflections from the L-KC should arrive at times ranging from 548 msec for vertical-incident traces to 610 msec for offsets of 900 m. Using this general relationship, the exact set of reflection wavelets returning from the injected interval can be identified on shot gathers.

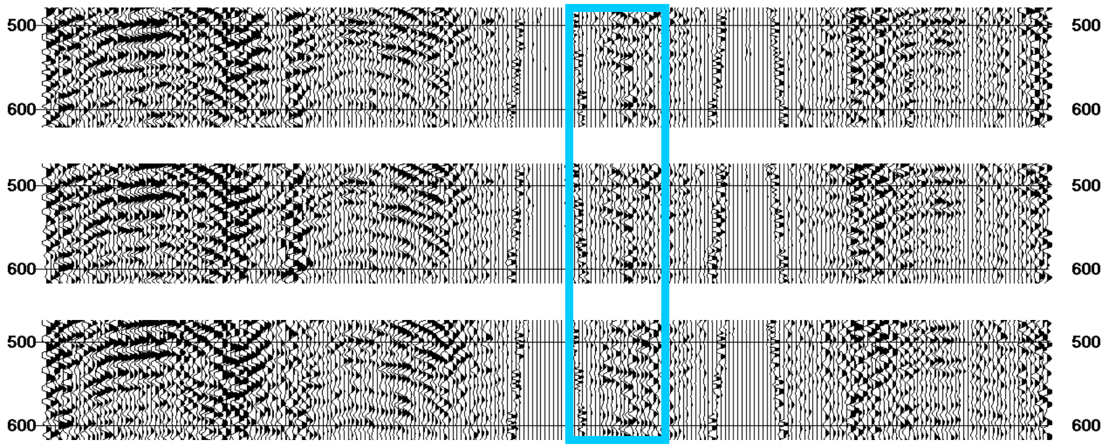


Figure 48. Time slice from the depth range of interest; baseline survey (top), first monitor survey (Jan. 2004) (middle), and second monitor survey (March 2004) (bottom). Clearly with the passing of time and increased volume of $CO_2$—the reflection evident within the box at approximately the correct time for the L-KC—appears to possess steadily increasing amplitude. This increased amplitude could be indicative of increased reflectivity resulting from changes in layer characteristics.

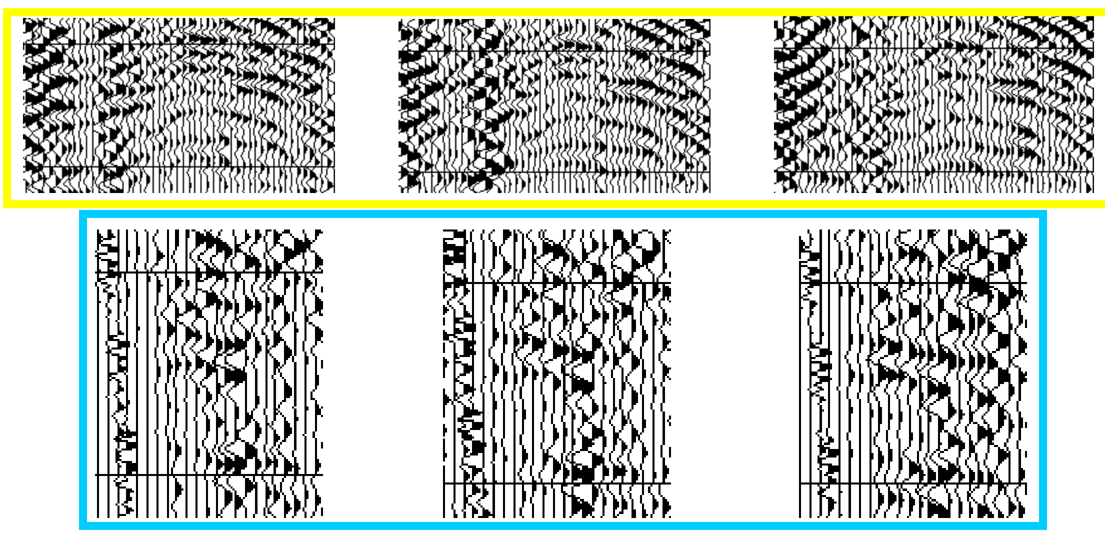

Figure 49. Magnified comparison of reflections within the time depth approximately correct for the L-KC interval. Blue and yellow highlights correlate to same zones in Figures 47 and 48.

Using the time-to-depth conversion extracted from the downhole survey conducted in #16 (Figure 50), it is possible to bulk time-correct the synthetic seismogram (Figure 51) for the normal inaccuracy in absolute time resulting from estimating overburden velocity. As usual, these errors range from less than a percent in areas with an abundance of ground truth to as much as 10 percent when no other information but the sonic log is available to help estimate replacement velocities. Using local well data only, the L-KC interval was estimated to be at a time depth of around 535 msec. Incorporating the VSP and manual wavelet-correlation techniques, the actual arrival time of the top of the L-KC on seismic data was around 548 msec. Using the VSP for the first-arrival information alone more than justifies the expense of getting these borehole data. Correlations between borehole and surface seismic were critical to accurately defining the wavelet returning from the L-KC. Considering the producing interval, and therefore the interval the $CO_2$ is being injected into, is only 15 ft thick and equates to just a little more than 1 msec, it is imperative to identify the L-KC reflection within a few tenths of a percent.

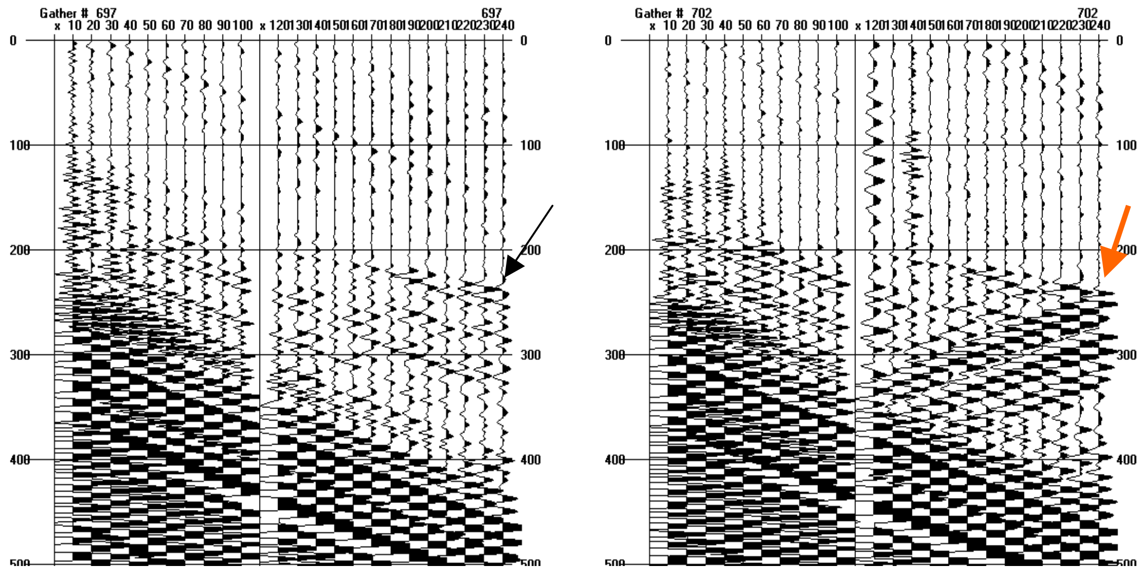


Figure 50. Uphole/VSP survey conducted in Colliver #16. ⟶ Indicates first arrival of seismic energy from source at hydrophone 2270 ft below ground. ⟶ Reverse energy is tube wave bouncing off weight hanging from bottom of cable carrying hydrophones.

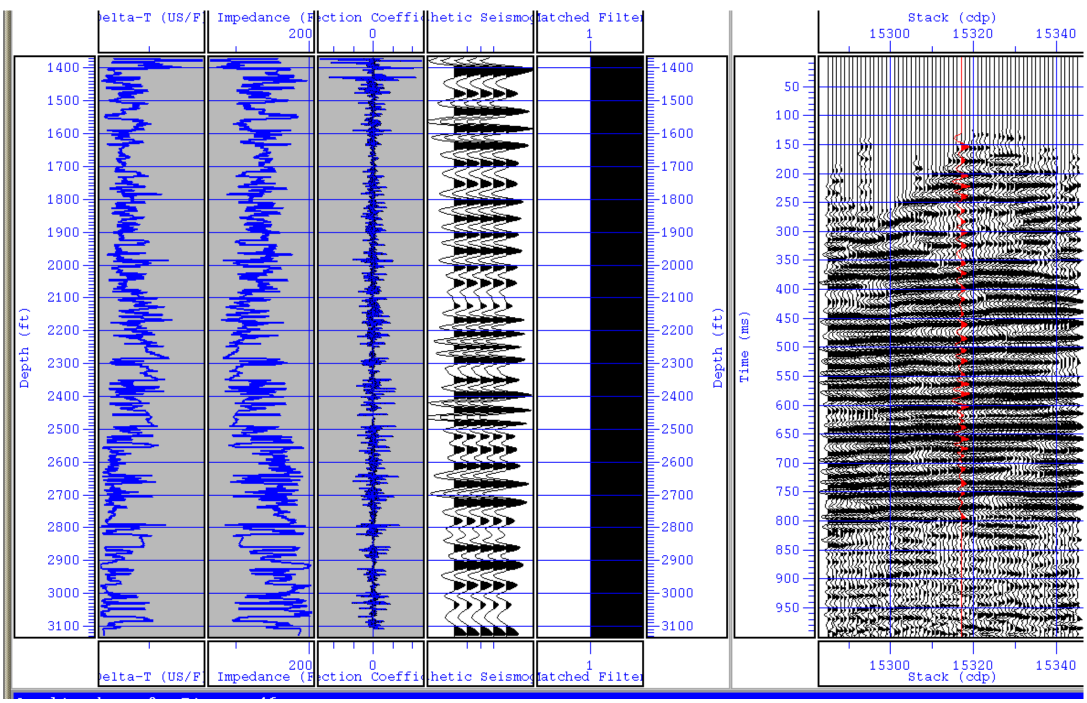


Figure 51. Synthetic seismogram generated from a sonic log from CO2I#1 convolved with a Klauder wavelet. The tie between the synthetic and real are outstanding at these lower frequencies. As spectral enhancements are complete the dominant frequency and resolution will increase significantly.

A 3-D seismic volume produced for the baseline survey provided an excellent look at preliminary data quality. At this very early stage of the data processing, reflection events looked quite good and only lack some of the sitewide coherency generally associated with seismic data from this depth interval and in this part of Kansas. However, considering the excellent data quality evident on shot gathers and with improved velocity analysis and statics, these data will provide the necessary quality to test the effectiveness of low-cost, minimal-deployment 3-D to monitor $CO_2$ injection from both the enhanced oil recovery and sequestration perspectives.

Over the period June 23-July 1 the third monitoring 3-D seismic survey was conducted to obtain a snapshot before the flood began a WAG (water-alternating-gas) program.

**Preliminary Processing and Interpretations** ***(To date the seismic data from the baseline survey [November 2003] and first two monitoring surveys [January and March 2004] have undergone preliminary processing and very rudimentary interpretations)***

Design of the receiver and shot grid was based on azimuth, offset, bin squareness, fold distribution, and equipment (Figure 52). Using the actual shot and receiver locations occupied, it was possible to improve slightly some of the grid characteristics. In particular, the fold distribution could be improved at the expense of centralization of midpoints within the bins. By rotating the grid slightly (Figure 53), the fold uniformity improved by almost 20% with only a minor increase in midpoint scatter within the bins as evidenced by the spider plots showing azimuthality and midpoint location (Figures 54 and 55).

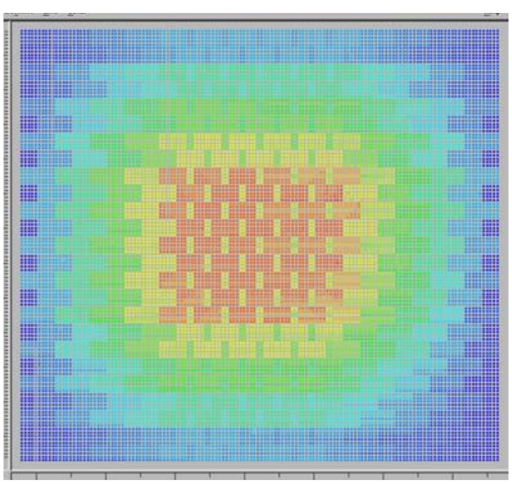

Figure 52. Fold map of grid (red-24 fold; yellow-20 fold).

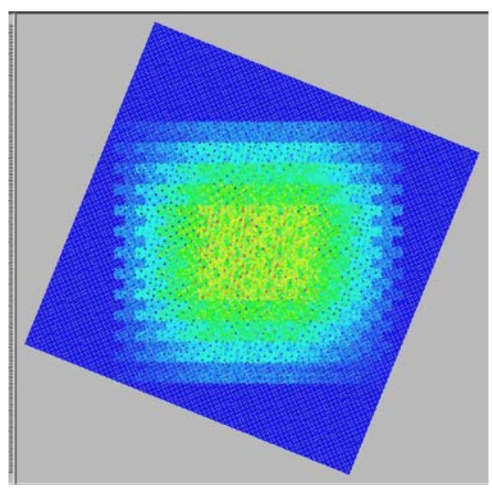

Figure 53. Grid rotated 112º.

Rotating the grid 112º (Figure 54) retained the squareness of the 10m x 10m bins and dramatically improveed the fold distribution. With every compromise comes a negative and for this improvement in fold distribution, midpoint scatter within the bins increased.  This scatter was evident in the spider diagram (Figure 55).  Even though this increased scatter in midpoint centrality was not an improvement, its effect on the overall detectability of the $CO_2$ front should be negligible and therefore had no impact on the objectives of this research program.

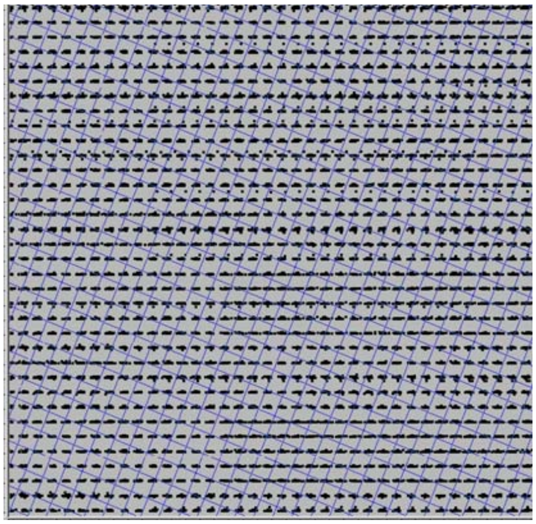

Figure 54. Midpoints and associated rotation.

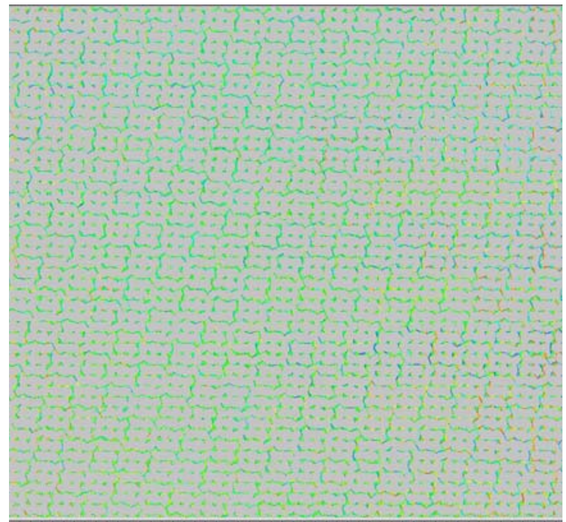

Figure 55. Spider diagram; midpoint azimuth.

Even at this early stage in the project, post-stack processing of the seismic volumes provided results that are both encouraging and somewhat unexpected.  Significant early pre-stack processing problems related to long-offset NMO stretch, multiples, statics, and reduced resolution for far offsets have been, for the most part, overcome. CMP stacked volumes now possess excellent coherency, with a well defined and detailed velocity function, and near-surface static problems have been all but eliminated (Figure 56).  Improvements in the processing flow and parameters are still being made, but the data are ready for preliminary interpretations, including some first-order attribute analysis.

Synthetic seismic data derived from sonic logs taken in wells CO2I#1 and #16 provided essential ties between time on seismic sections and depth on borehole logs. Preliminary correlations between synthetics and real data have been excellent, with convincing matches between the real and synthetic seismic data in proximity to CO2I#1. Once the higher frequency reflections are enhanced and the dominant frequency moves over 100 Hz at the target depth, final synthetics will be produced allowing identification of the L-KC “C” to an accuracy of around one sample or 10 ft.

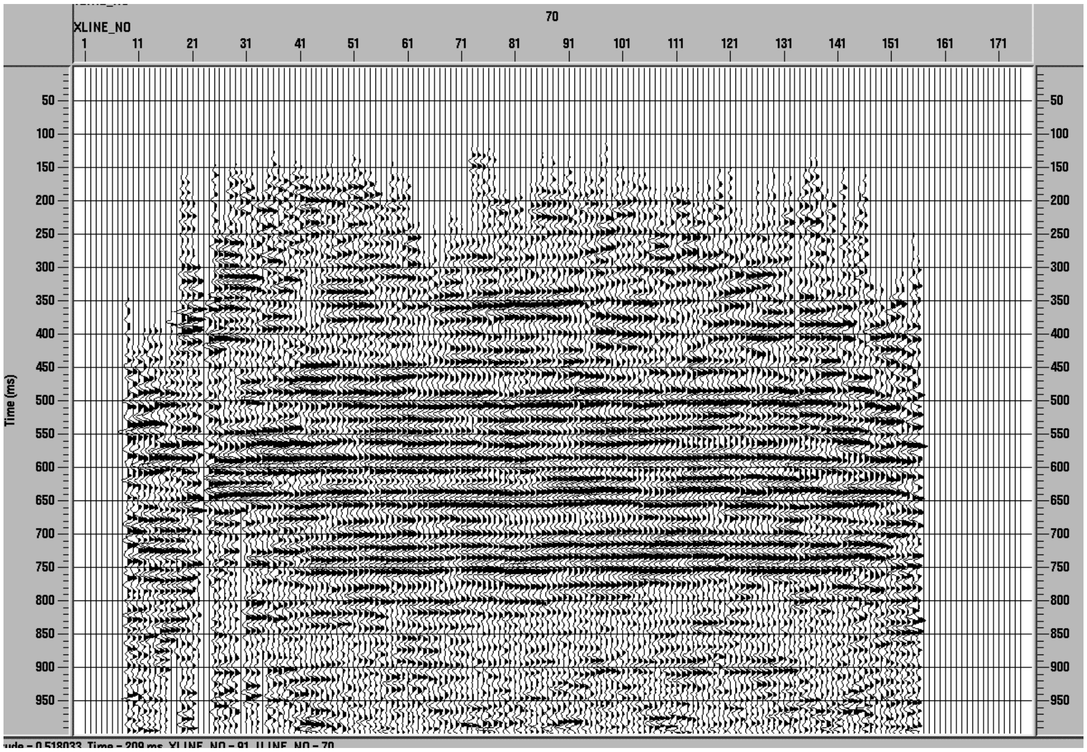

Figure 56. 2-D CMP stacked section extracted from 3-D volume of the second monitor survey. Reflection coherency is very good. Improvement in bandwidth and coherency of shallower reflections will be the primary focus of the next round of processing enhancements.

Key to many seismic analysis techniques and essential for attribute analysis is the preservation of amplitude, frequency, and phase of the reflected signature. All contributions from the seismic source and noise sources must be reduced as much as possible and ideally eliminated. The reflection signature left on CMP stacked sections must have characteristics that are as closely related to the reflected interface alone as possible without contributions from source, near surface, or background noise (both random and periodic). Considering the comparatively close offset range of interest for these relatively shallow reflections (by industry standards), a significant amount of ground roll and air-coupled wave was removed during processing, leaving some CMP bins with very low fold for some near offset ranges. Removal of multiples is also an important step for optimizing the analysis of these data, because changes in reflection characteristics related to the presence of $CO_2$ in comparison to reservoir fluids are small (~2-20% percent). These data have undergone an extensive series of noise reduction steps to maximize the signal-to-noise ratio and statics/velocity corrections to improve coherency (Figure 57). More work needs to be done to verify that key attributes (phase, frequency, and amplitude) have been preserved up to this point in processing.

Instantaneous attributes are measurements of specific seismic properties at an instant in time. Measurements of this type are only reliable and useful in extracting meaningful geologic characteristics if all phase and amplitude information is preserved during processing. Multiples and random noise limit the accuracy of interpretations derived from instantaneous attributes.

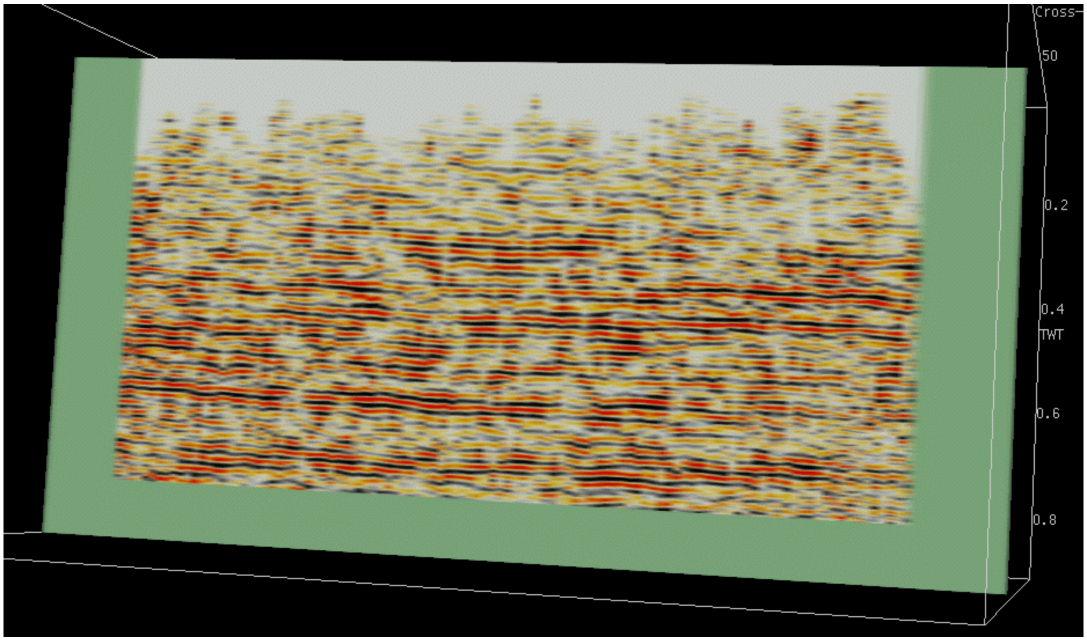

Figure 57. 2-D slice of 3-D volume with wiggle trace amplitudes represented in color. Coherency is quite good, but work is still underway to insure true amplitudes have been preserved through all processing steps. A few amplitude anomalies resulting from previous work eliminating noise can still be observed on this section.

Given the areal size of the site, it is important to consider the horizontal resolution of the data in interpretations of map view representations of instantaneous attributes. Using the Fresnel zone as the basis for establishing horizontal sampling size on a layer, at 2,900 ft below ground surface for the observed frequencies the radius of the Fresnel zone (generally assumed to be the wavelet sampling size) is approximately 350 ft. Bin dimensions for these attribute data are approximately 30 ft x 30 ft with a unique value for each cell that includes variable contribution from the surrounding 50 or so cells or ~5 cells away in any direction. Therefore, even though the greatest contributions to each cell's value are from rocks within that cell area, nearby rocks outside the bin influence this value to some degree. Interpretations of patterns or textures must consider the overall sampling size of the wavelet and how far from the cell changes in rock property contribute to the overall signature.

In this document well locations are based on conversions from legal descriptions assigned during the permitting process when the wells were initially drilled. Therefore exact plotted locations relative to this DGPS (± 0.25 m) seismic grid could be in error by 50 ft or more (up to several cells). DGPS locations of the wells were obtained following the third survey and will be utilized in future analysis but are not shown in the figures here.

Interpretation of the seismic response, particularly for reservoir properties and fluid property changes, involves analysis of numerous attributes of the seismic waveforms returning from the subsurface and specifically from the single wavelet (peak and trough) that sampled the L-KC "C" zone. With only the uphole data from #16 available (synthetics and VSP are not fully developed yet) for time-to-depth correlation of reflections with reflectors, it is not yet possible to confidently identify the exact wavelet returning from the L-KC "C." When the synthetics are fully developed and confidently matched with the real data, the exact reflection horizon corresponding to the "C" zone will be mapped and attribute analysis will be performed specifically on the "C" zone reflection. Analysis to date has identified a zone or layer 24 msec (100 ft) thick, which includes the horizon of interest. Preliminary post-stack analysis of the seismic time-slice calculated to contain the "C" zone has been performed to investigate and uniquely identify any changes in response within this volume between the baseline and the subsequent two monitor surveys.

Instantaneous amplitude (amplitude constant-time slice) is the most intuitive of the instantaneous attributes; it provides a measure of reflectivity that represents a map view of seismic amplitude changes. In the case of these 3-D seismic volumes, an instanttaneous amplitude time slice provides a general measure of layer structural/depositional topography more than reflectivity, assuming the velocity along the time slice does not vary significantly. From well data within the 4-D seismic area, the L-KC "C" zone exhibits approximately 35 ft of relief between a low near Colliver #6 and high near Colliver # 8. Structurally, Colliver #5 and #6 (west end of survey area) are drilled into lows and Colliver #16, #13, and #8 (eastern end of survey area) are all in a relatively high area. In general, these changes in elevation measured in the well bores are consistent with the amplitude trends on the 560 msec amplitude time slice (Figure 58). Considering this is a time slice and not a horizon map, variations in color are most sensitive to movement of the wavelet up and down in response to changes in reflector depth with only minor contributions from changes in layer reflectivity. Correlation between L-KC "C" elevation and amplitude values is excellent. Work continues trying to map geological/ rock-property discontinuities using seismic continuity/similarity volume attributes, which highlight geological discontinuities potentially affecting $CO_2$ movement through the reservoir.

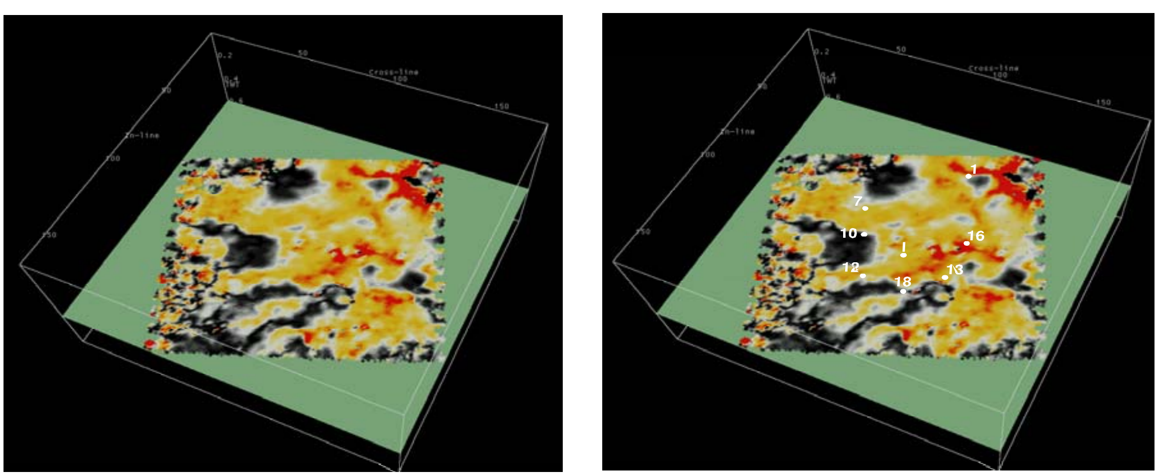


Figure 58. Color representation of amplitude values along the 560 msec time slice. Dark areas are relative lows and reds are structural highs trending into yellows representative of intermediate depths.

During final data analysis many different visualizations will be necessary to interpret the subtle changes expected from replacement of reservoir fluids (oil and water) with $CO_2$. In-line and cross-line seismic sections are used to calculate various seismic attribute volumes and provide the anchor for studying changes in key time slices and horizons throughout the volume. This analysis approach provides the 3-D visualization utilized to track $CO_2$ movement and geological spatial extent of structural, stratigraphic, and lithologic seismic signatures (Figure 59). Data coherency and uniformity in amplitude characteristics are excellent throughout the interval of interest. Processing to date has focused on the 400-to-700 msec time/depth window. As is evident on shot gathers, many reflections were recorded both shallower and deeper than this interval, and these extraneous reflections will be the target of enhancement processing once the preliminary analysis is complete on the principle zone of interest.

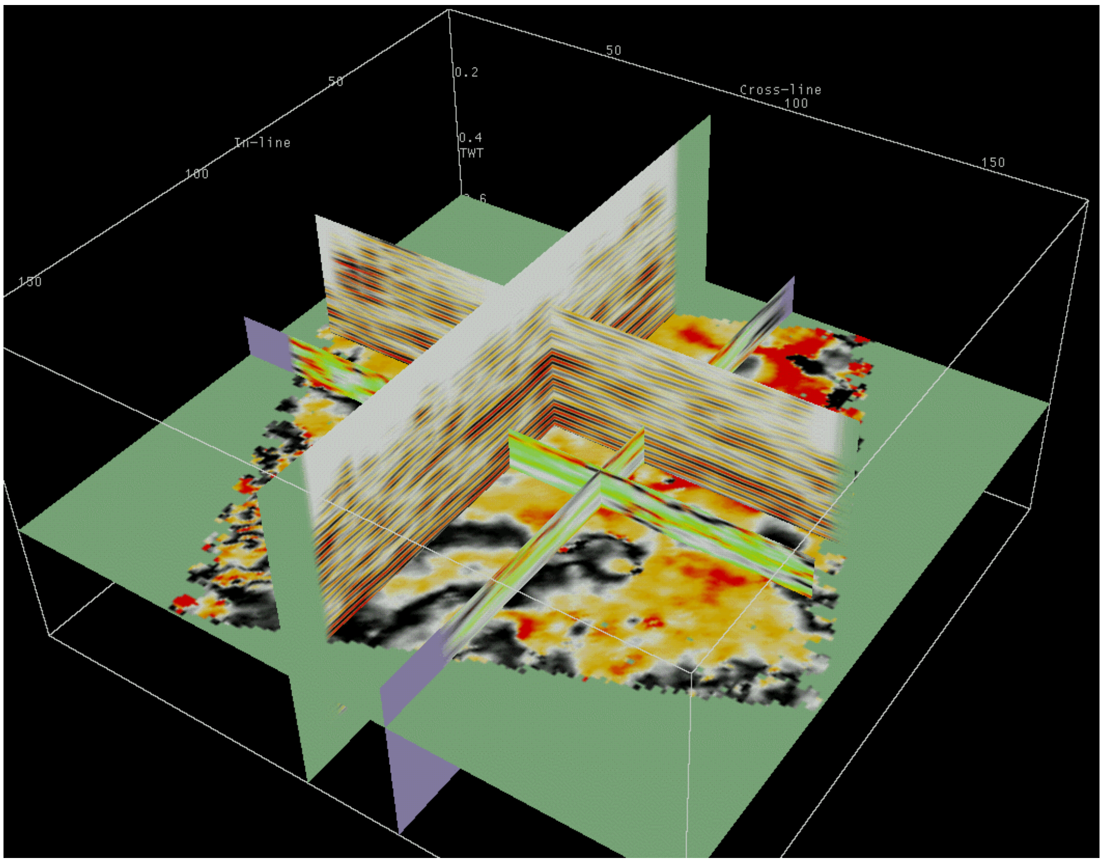

Figure 59. Vertical cross-line and in-line color wiggle trace displays intersected by the 2-D time slice from near the L-KC “C” interval. Correlating the time slice with reservoir tops as defined by well logs results in an excellent match between structure and amplitude. Reds are structurally higher than yellows, which are then higher than the blacks. Average instantaneous frequency in-line and cross-line sections (low is green and high is red) for a sub-volume around the target zone is shown.

Preliminary processing of the first three surveys (baseline and two monitor) has provided crude time lapse analysis and shows changes between the baseline survey and the two surveys obtained after $CO_2$ injection began in December 2003. Some of these changes in seismic response can be interpreted to relate to changes in reservoir properties. As noted, with only the uphole data from #16 currently available for time-to-depth correlation of reflections with reflectors, it is not yet possible to confidently identify the exact reflection wavelet that has returned from the L-KC “C.” However, a zone or layer

24 msec (100 ft) thick has been selected that includes the horizon of interest. Since the zone of interest (L-KC "C") is only 15% of the total thickness (15 ft of the 100 ft thick time slice) being analyzed, and the change in reflectivity associated with the fluid change from water/oil to $CO_2$ is expected to be less than 20%, changes in seismic properties resulting from the presence of $CO_2$ should be less than 4%. A change in the seismic response this small is at the detection limits of this thick slice analysis technique. It is therefore imperative for accurate interpretation that the exact horizon of interest be identified and analysis be focused on that interval.

A critical processing step that has yet to be performed on these seismic data is equalization. Ground conditions—and therefore coupling and velocity—change over time, resulting in data differences related to what is happening <u>on</u> the ground rather than <u>in</u> the ground. Even with the extreme care taken during acquisition to insure all equipment, parameters, and station locations were identical between surveys, minor changes in surface conditions between the different data acquisition campaigns affect each data set differently. Therefore, corrections unique to each survey data set must be made to reduce and hopefully eliminate surface effects that vary with climate from subsurface effects. After equalization, characteristics of resulting data sets can be directly compared and differenced data sets can be used to highlight $CO_2$ movement. It is important to note that since the data equalization processing has not been completed some of the differences observed between surveys are likely from changes in surface conditions and not changes that occurred in the subsurface.

Instantaneous frequency (IF) analysis was performed on the 24 msec-thick seismic volume. IF is an attribute sensitive to the temporal change in the continuity of seismic events, specifically; it is sensitive to waveform characteristic changes resulting from velocity and/or thickness variations in a thin layer. In general terms it can be considered a measure of seismic spectral attenuation within a rock layer. IF plots by nature tend to have a high degree of variability. Although lateral changes in rock lithology are detectable using IF analysis, numerous different kinds of lithologic changes can produce IF features or anomalies and it can be difficult to interpret the nature of the lithologic change responsible. Because IF is more sensitive to noise and changing patterns of noise than most other seismic attributes, it is advisable to use the multiplicity/redundancy of 3-D seismic sampling for a spatial averaging-extraction strategy, thus reducing the percentage of noise-related random variability in IF. This study has the benefit of multiple time-lapse images of the zone of interest. Changes in IF "texture," or the development of unique patterns on time-lapse images, may provide a good indication of small fluid composition changes within the layer itself, particularly when it is spatially continuous and consistent in a 4-D sense. As noted, these surveys are not equalized, and considering this analysis technique is especially sensitive to noise, changes in color patterns or textures on these plots can be partially a function of data equalization issues (changes in the near-surface not fully compensated for during processing or changing patterns of noise).

Parameters selected for displaying the IF plots were optimized for the baseline survey data (Figure 60). A specific color scale tuned to minimize the expression of variability while enhancing differences across the time slice was selected for all displays. Using this approach, coherent changes in IF that develop over time should be evident. Considering the expected change in seismic properties with the 24 msec time slice as a result of a change in fluid composition from water/oil to high-pressure $CO_2$ for the seismic volume being analyzed is less than 4%, as much visual enhancement as possible is important. Again, noting that some differences may be related to equalization and pressure changes in the pattern, development of consistent patterns or local changes in texture are likely indicators of $CO_2$.

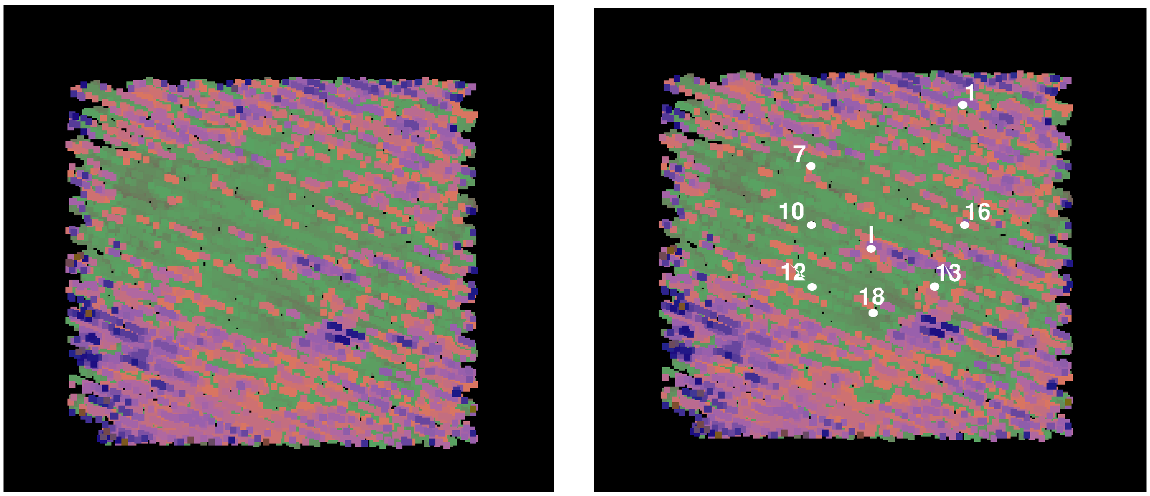


Figure 60. Baseline Survey—Color representation of instantaneous frequency for a 24 msec-thick slice at a depth of around 560 msec for the baseline 3-D survey conducted when the field was fully pressurized with water and just prior to the first injection of $CO_2$. Well locations (coordinates based on conversions from legal descriptions) are placed to improve spatial awareness of the key locations around the field.

An obvious northwest to southeast grain is evident in the IF plots. This grain is the result of rotating the grid 120° during processing to improve the distribution of sub-surface samples. Values in each cell are independently calculated from CMP traces within that cell only and are in no way influenced by CMP traces gathered within adjoin-ing cells. Therefore, the discrete, blocky character of the displayed data is a result of the receiver line orientation (trends along inline direction) and rotation of the seismic bins.

Some sense of the lithologic trends potentially influencing the performance observed at the various wells can be gained by comparing and contrasting apparent boundaries and changes to the texture of specific seismic properties across the site. In making these observations keep in mind that both the amplitude and frequency attribute plots (Figure 61) show response changes for seismic volumes representing an interval of rock over 100 ft thick that includes the subsurface interval of interest. Thus some of the data characteristics observed may be from overlying and underlying beds, or changes in the "C" zone may be subdued by consistent seismic response from overlying and under-lying beds. A prominent feature evident in both plots is a contrast in properties north and south of an east/west trending line (A) lying immediately south of well #18 (Figure 61). This trend (A) marks a substantial change in seismic character on both amplitude and frequency plots and may indicate the presence of a structural feature or an abrupt change in rock properties. Another lineament (B) follows a high (red) trend on the amplitude plot and an anomalous group of cells on the frequency plot. This feature, though subtle on both plots, is interpreted to exhibit sufficiently high contrast to represent a marked change in rock properties of some kind. A third more subtle northeast/southwest trending lineament (C) marks a change in texture on the frequency plot and an apparent alignment of anomalies on the amplitude plot. Because of the greater sensitivity of instantaneous frequency to lateral lithologic changes in comparison with instantaneous amplitude, it seems likely this (C) lineament may be related to a lithologic change. It is unlikely the (C) lineament would have been interpreted from amplitude plots alone.

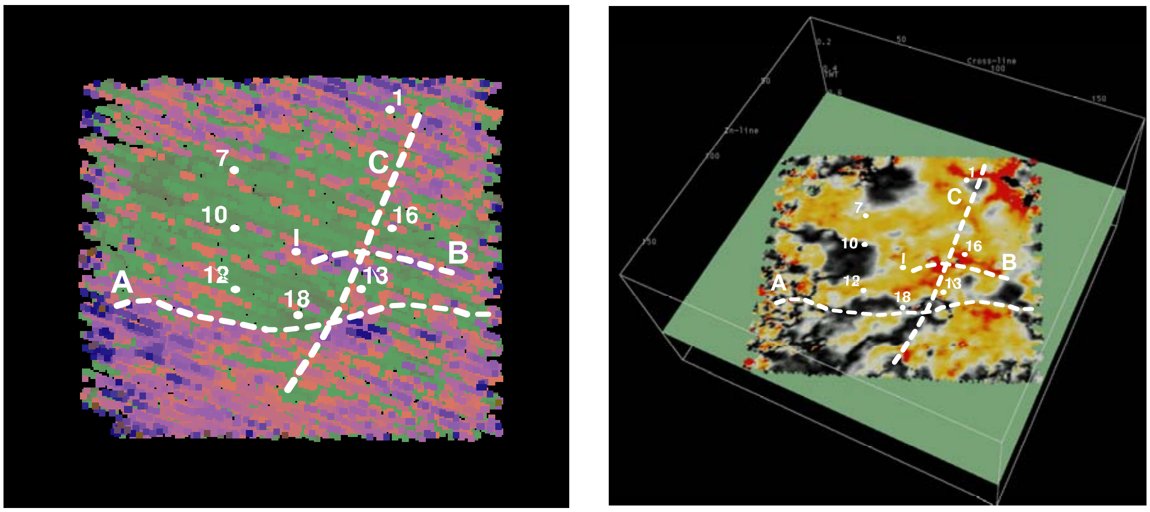

Figure 61. Baseline Survey—Lineaments based on changes in data character or texture were interpreted on baseline data from 24 msec time slices at around 560 msec. These lineaments are interpreted identically on both lines—instantaneous frequency (left) and amplitude (right).

Analysis and comparison of the baseline and first and second monitoring surveys show changes in instantaneous frequency within the study area (Figures 60, 62, and 63). Because of the thickness of the seismic volume, equalization, and IF response issues, interpreting these data at this stage will be limited to identification of areas where changes occur between surveys. All significant changes observed in these data are generally within an area defined by wells number 12, 18, 13, 16, 7, 10, and 1 (Figure 64, "b" or right side). Comparing and contrasting the two monitor surveys with the baseline survey, changes in IF can generally be grouped in one of four ways: 1) similar change in both monitoring surveys, 2) change in the first survey not evident on the second survey, 3) change in the first survey and a different change in the second survey, and 4) no change in the first survey but change in the second survey. The third monitoring survey obtained June 23-July 1 will provide a further examination of the consistency of changes in different areas. Definition of the LKC "C" zone wavelet will also refine changes.

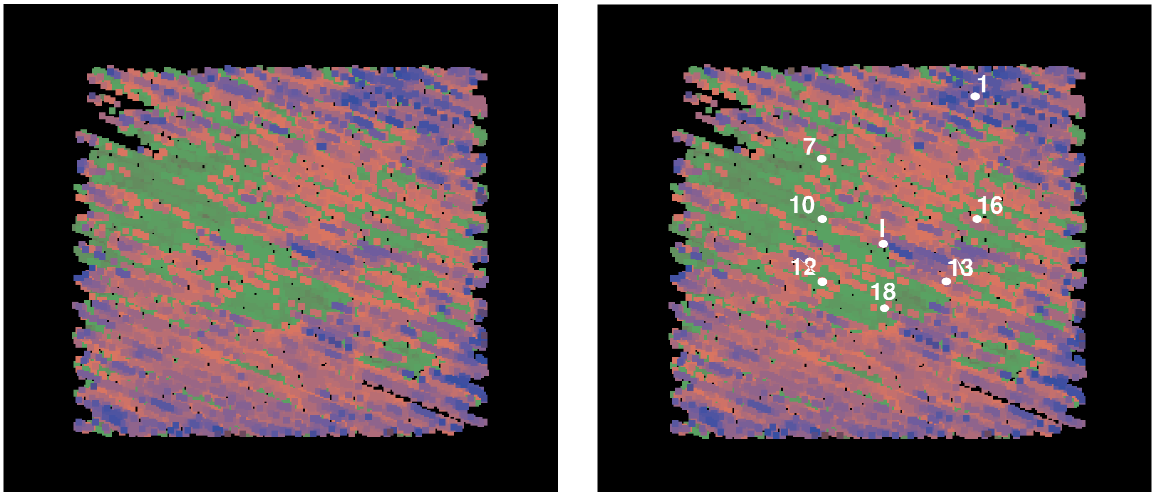


Figure 62. First Monitor—Instantaneous frequency plots of the first monitor survey using an identical color scale as used on the baseline (left). Well locations are estimated from conversion of legal descriptions, so some inaccuracy exists in their locations (right).

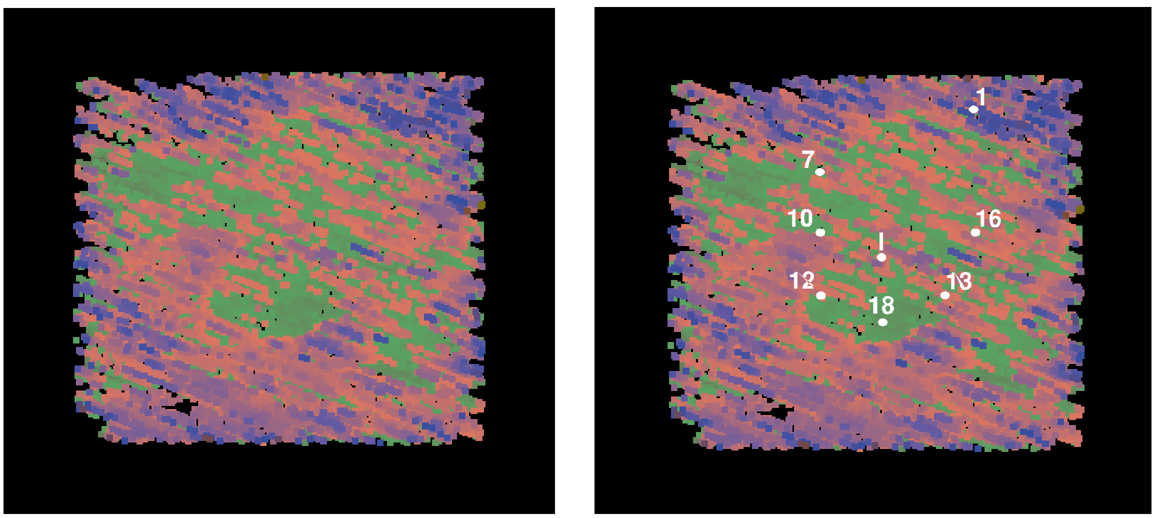


Figure 63. Second Monitor—Instantaneous frequency plots of the same 24 msec time slice as displayed for monitor survey one and the baseline survey. Color scales and well locations are identical for all IF plots.

The evident changes in texture for the general $CO_2$ pilot region compared to outside the flood region lend support to the idea that changes are being detected. However, interpretation of the causes for the differences observed between the monitor surveys is not yet clear nor is the size of the area of change in the subsurface compared to the seismic response fully resolved (Figure 64). Volumetric analysis precludes the possibility that change observed in the entire region shown in Figure 64 represents significant $CO_2$ invasion. Assuming $CO_2$ was flooding only a 1-foot thick interval with the $CO_2$ displacing only 33% of the oil/water in the pores, the change observed only in the northeastern quarter may be due to $CO_2$ invasion at the time of the first monitor survey (Figure 64 Bb). However, this would require that $CO_2$ moved along a focused region or arc and did not move radially out into the formation from the CO2I#1. Insufficient $CO_2$ volume was injected at the time of the first monitor survey to affect the entire area simultaneously. However, seismic response will noticeably change with a small percentage change in saturation of $CO_2$. As well, considering the size of the Fresnel zone, "fingering" will appear enlarged on seismic data. Depending on the geometry of the "fingering," seismic images could easily represent thin zones of higher $CO_2$ saturation that are moving through the reservoir**.**

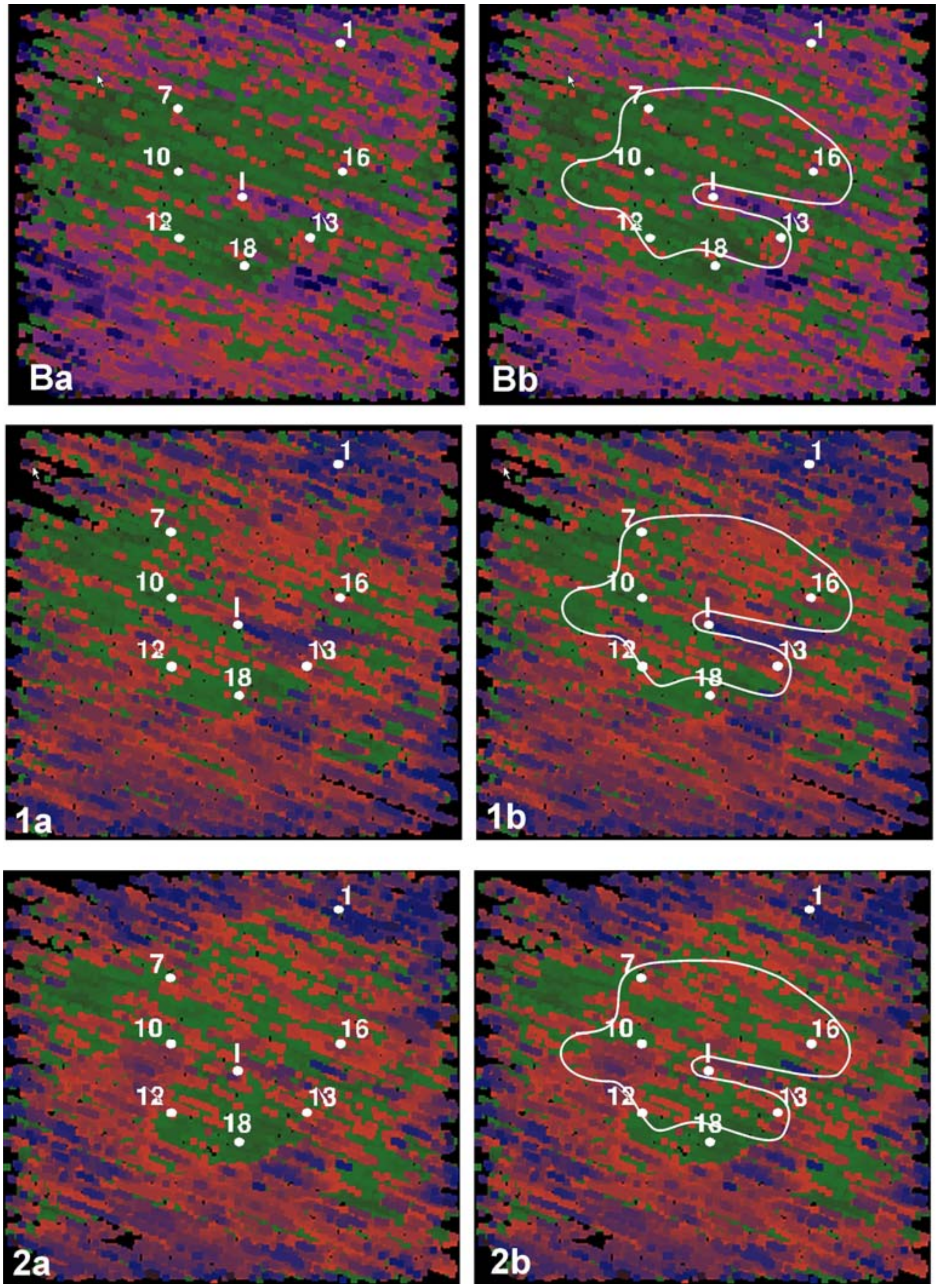


Figure 64. Comparison of baseline (B), monitor 1 (1), and monitor 2 (2) IF plots with wells located (a). The area highlighted possessed notable changes in data character, intensity, and/or texture between the three surveys. Changes between surveys are not necessarily consistent due to a variety of reasons (equalization, changes in reservoir, etc.), but the changes observed within the highlighted area seem to suggest that as the $CO_2$ has progressed the subsurface in proximity to the injector is experiencing changes.

In general changes on the monitor surveys relative to the baseline survey are predominantly north of CO2I#1 (Figure 66). Changes are evident south of CO2I#1 but they appear less coherent as a mass and seem to generally increase in areal extent on the second survey relative to the first. When considering the extremely small percentage change expected in seismic properties of the L-KC "C" for this study, changes from one monitor survey to the next on these particular preliminary analyses might not be numerically consistent. Areas consistently changing rather than consistent change relative to the baseline survey are the targets of the seismic attribute analysis at this point in the interpretations.

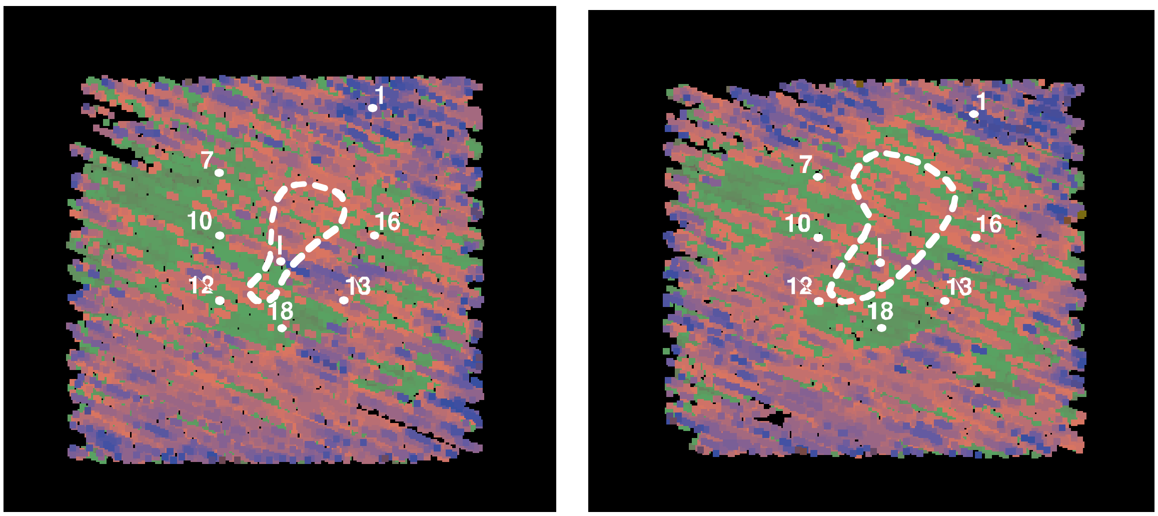


Figure 66. Monitor survey one (on left) and monitor survey two (on right) with the areas possessing the greatest and most consistent change relative to the baseline survey outlined with a dashed line. These areas of greatest change are not necessary numerically consistent with each other, but they do, from a relative perspective, contain the set of cells that define the greatest overall relative change.

**<u>Seismic Data Acquisition: Monitor Survey Three</u>**

With initial $CO_2$ detected in Colliver #12 near the end of May, this third monitor survey provided an important snapshot for reconstructing the time-lapse path $CO_2$ has taken through the field from injector to producer. Based on pre-injection models, progression of $CO_2$ from injector to producers as well as the volumetric expansion of the $CO_2$ slug was expected to preferentially move toward Colliver #12.

This third survey was delayed a few weeks until after wheat harvest, avoiding significant damage to the wheat crop being grown on about one-third of the survey area. On June 25 the wheat harvest was completed. An unusually rainy June also delayed acquisition by several days. Ground conditions were ideal for receiver coupling immediately after harvest with only wheat stubble left in the fields (noise from wheat moving with the wind was all but eliminated) and because of the 3+ inches of rain that fell the week before the start of the third monitor survey (Figure 66). A negative aspect of these ideal receiver conditions was the softer-than-previous ground conditions, which with a vibrator source reduces the efficiency of the energy transfer process.

Figure 66. View looking west showing vibrator sweeping in the wheat stubble field surrounding the $CO_2$ injection well. Colliver #12 is visible on the horizon to the left of the vibrator in this picture. The $CO_2$ injector is enclosed in a yellow steel protection fence and can be seen immediately behind the vibrator, in the distance. Combines completed cutting wheat from this field just days before this picture was taken.

Surface conditions changed between the end of March and end of June surveys. Geophone planting conditions were very similar while surface activity and associated noise was quite different. Noise from cattle and farm equipment provided new challenges to data acquisition and processing. Cattle were penned away from the receiver lines but we were still were close enough to be a source of noise on the northernmost receiver line (Figure 67 left). This third monitor survey was scheduled as soon as possible after the second monitor survey while avoiding wheat harvest, rain, and the plugging of Colliver #2 (Figure 67 right).

Figure 67. Noise sources and unique acquisition obstacles change with each survey and the seasons. (left) Cattle in the pasture immediately north of the $CO_2$ injector. (right) Colliver #7 pumping in the foreground and Colliver #2 being plugged in the background.

Ground and weather conditions were ideal during the first several days of acquisition. With over three inches of rain falling days prior to the deployment of receivers, planting and coupling conditions were very good and better than expected for this area during this time of the year (Figure 68 left). Geophone locations were DGPS surveyed to be within a few centimeters of previous geophone locations. Because the wheat had just been harvested the cables could be laid quickly through the stubble with ATVs, reducing the extra care necessary on previous surveys to minimize damage to growing crops (Figure 68 right).

Figure 68. Geophones were planted (left) in a 0.3 m equilateral triangle centered on the DGPS-located station. Weatherproofed reenforced Ethernet cables stored on spools (right) connected the eleven 24-channel Geometrics Geodes to the NZC seismic controller. These cables were deployed using a custom cable handling system.

Shot gathers from this survey were of similar quality to those from the previous three surveys (Figure 69). Wind was light and variable with speeds not exceeding 15 mph. Noise from the fixed sources (pump jacks, pipelines, and power lines) is evident as on previous surveys. Vehicle noise on county roads was random, but was overall equivalent in volume and frequency to previous surveys as well. Unique to this survey was the noise from cattle movement near line 1 and the combine harvesting wheat on June 25 near the east end of lines 3 and 4. Contributions by both these noise sources, new to this third monitor survey, were minimized due to their non-stationary nature and the collection of four-sweep vertical stacks at each station.

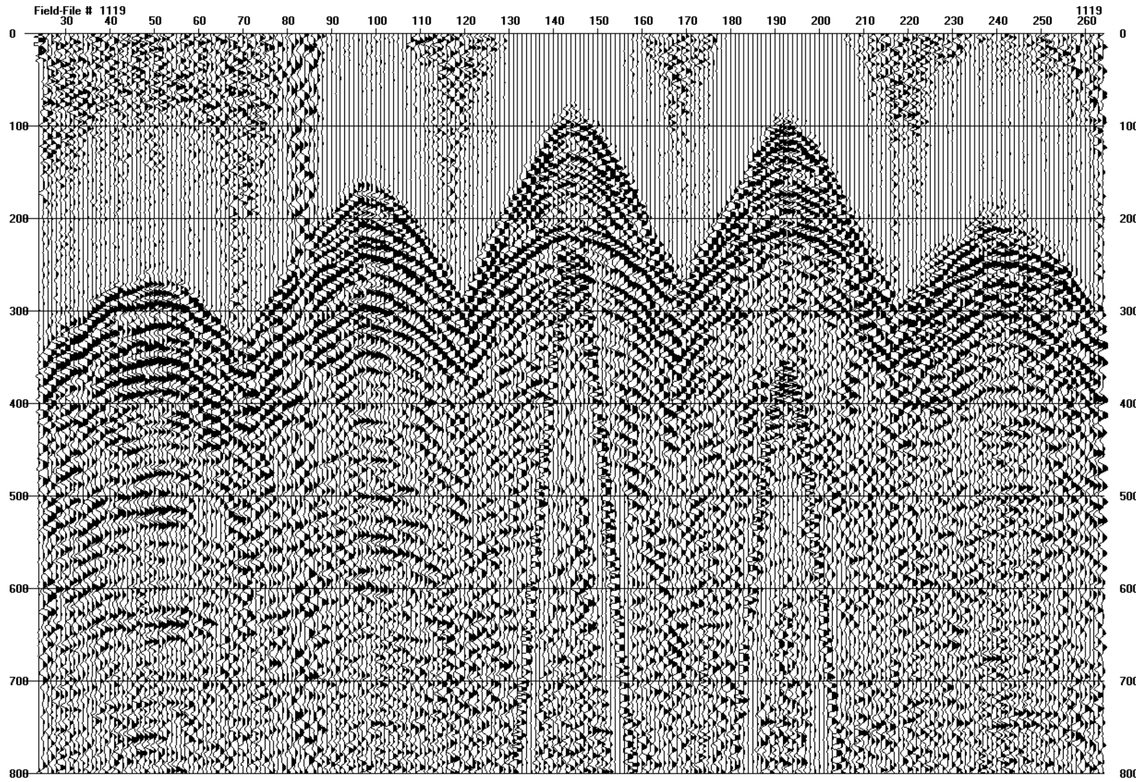


Figure 69. A single sweep from near center of the receiver spread. This shot gather has been scaled to enhance reflections within the 2500 to 3500 ft depth range. Reflections from the L-KC "C" zone will arrive between 550 and 650 msec across this spread. This range of arrival times is directly related to source-to-receiver offset and associated non-linear increase in travel path with source-to-receiver separation.

An apparent dominant frequency of around 120 Hz at 1,000 ft and 60 Hz at 3,000 ft was increased by 50% at 1,000 ft and doubled at 3,000 ft during processing using spectral balancing techniques (band-limited spiking deconvolution). Vibrator ground force was around 12,000 lb at 60 Hz, decreasing linearly to around 6,000 lbs at 200 Hz. Spectral properties of the recorded data were controlled by the source energy spectrum (power as a function of frequency) and the natural attenuation of higher frequencies by the earth. With large dynamic range recording systems and minimal background noise, low amplitude signal at higher frequencies were enhanced to some degree relative to the more dominant lower frequency recorded energy.

Data quality on this fourth survey (third monitor survey) was not quite as high as on the previous two monitor surveys. Considering the efforts taken to insure exact duplication in equipment and parameters, this difference was clearly related to the ability of the ground surface to accept and propagate seismic energy (Figure 70). The noticeable enhancement in coupling between receivers and the ground was likely due to the substantial rainfall that preceded the survey. Unfortunately the softer ground conditions that resulted from the rain adversely affected energy transmission by the source into the ground. Ground force curves, as calculated using the baseplate and mass accelerometers, were consistent with previous surveys, while the recorded energy levels at the receivers were down. The difference was clearly related to the saturated nature of the upper 1 ft of soil in this area.

Figure 70. November survey (upper left), January survey (upper right), March survey (lower left), and June survey (lower right).

Data acquisition for this third monitor survey required eight days with an additional two days of land surveying to relocate receiver stations after wheat harvest was completed and cattle were put out to graze across part of the survey area. An additional day of surveying was necessary to exactly locate the wells within the survey grid. With another almost two inches of rain falling the night after the final sweeps were recorded for this survey, small footprint, low ground-pressure vehicles kept the equipment free of excessive mud and avoided damage to farm fields and pastures (Figure 71). Equipment was picked up and the site secured in a day.

Figure 71. With almost two inches of rain the night after acquisition was complete, the six-wheel drive ATVs were instrumental in picking up and transporting cables and phones back to the semi-trucks where they were loaded for transport back to Lawrence without “rutting” the farmer’s fields and pastures.